CONSTRUCTION AND TESTING OF A 600 kW BURNER FOR SAWDUST IN SUSPENSION

Lucian Mihăescu, Prisecaru Tudor, Manuela Elena Georgescu, Gheorghe Lăzăroiu, Oprea Ion, Ionel Pâşă, Negreanu Gabriel, Pop Elena, Viorel Berbece

„POLITEHNICA" University of Bucharest, 313 Sp. Independenței st., 060042 Bucharest E-mail:

Rezumat : Pentru puteri termice mai mari de 500 kW arderea în suspensie a rumeguşului reprezintă soluția cea mai adecvată. Se au în vedere în special aspectele legate de uşurarea alimentării cu rumeguş, care devine total pneumatică. Un cazan cu ardere în suspensie este mai simplu şi mai uşor decât unul cu ardere pe grătar.
Cuvinte cheie: ardere rumegus, cazan cu ardere în suspensie.

Abstract: For units having a thermal power higher than 500 kW, the suspension burning of the sawdust is the most adequate solution. There are certain aspects to be considered regarding the ease of feeding of the sawdust, which becomes fully pneumatic. A suspension burning boiler is simpler and lighter than one with grate burning.
Keywords: sawdust burning, suspension burning boiler.

1. USAGE POSSIBILITIES

When burning solid biomass (in the form of sawdust) some difficulties arise due to the rate of the density to the mass flow required for producing a certain thermal power. Subsequently, when burning in a layer, the air admission is somewhat difficult for a correct distribution to the entire quantity of biomass existing in the furnace. As a rule, for the layered burning, even when using sawdust briquettes, the thermal power of 1 MW per unit cannot be surpassed. The heating of large volume buildings is considered, especially for agricultural farms or for greenhouses.

A humidity value higher than 20% worsens the ignition and inhibits the burning process. There is a direct connection between the humidity and the endurance of the power installations, represented by the excessive fouling of the furnace and its convective part. The suspension burning increases from 2.5 to 3.5 times the boiler installation endurance, due to the intensified burning.

The solutions to solve these difficult aspects of the energy valorization of the biomass represented by the forming of biomass pellets dried in a hot air current, to a 6-8% humidity value, have higher costs and cannot be applied to units of high thermal power.

For units having a thermal power higher than 500 kW, the suspension burning of the sawdust is the most adequate solution. There are certain aspects to be considered regarding the ease of feeding of the sawdust, which becomes fully pneumatic. A suspension burning boiler is simpler and lighter than one with grate burning.

While in the field of energy valorization of wooden biomass by means of densification there are some achievements, the field of the suspension burning of sawdust is still in the incipient phase. That is because of the carrying of the sawdust particles to the flow limit of the air current (similar the pulverized burning of coal), by means of swirling burners.

Romania has a great potential for biomass (circa 14.5 million tons which can be energy valorized), but it has only partial achievements, especially in the field of burning technology with fixed and mobile grates.

This paper takes into account the influence of the new ecological fuel vector, with burning with floating in the air, on the quality of the ash resulting from burning. The new ecological fuel vector comprises the binomial: carrying air – particles form of solid biomass. The increase in the burning velocity permits the reduction of some pollutant components. If K_2O and CaO presence is reported in ash, the biomass ash could be considered to be an agricultural fertilizer and not a residual waste which must be stored away.

The testing objective is to achieve a complete and an ecological burning. Burning solid biomass, regardless of the technologies developed up-to-date, have the disadvantage of a

great carbon monoxide emission. By means of completely carrying of the solid biomass by the burning air current, inside an adequate height furnace, a massive reduction of carbon monoxide emission is estimated.

The increase in the burning velocity also reduces the fouling effects on the final heat exchangers of the power installations, contributing to the increase in the endurance of such installations.

From the social perspective, these achievements come to help the rural communities, which, with local renewable resources, could produce electricity and heat, with a competitive efficiency, similar to that on the energy market.

Automation is a defining component for the technology of suspension burning of the sawdust, imposing higher costs for the internal services (pumps, fans, feeders, etc.). As a result, besides the thermodynamic efficiency, the notion of economical efficiency is defined by:

$$\eta_{economic} = \frac{C_{et}}{C_{comb} + C_{ce}} \cdot 100, \%$$

where: C_{et} – is the cost of the energy produced, C_{comb} – the cost for the fuel, C_{ce} – the cost of the internal services electrical energy. The operator cost is not considered since the boiler is to be fully automated. An important part in the fuel cost is that connected to the storage and to the transportation. These economical calculations are necessary in determining the costs of the heating of spaces using biomass.

2. THE BURNER CONSTRUCTION

In principle, an installation to burn sawdust in a pulverized state has the following components: a fuel bunker, for an autonomy range of 4 to 6 hours, a pneumatic system to feed the sawdust to the burner, a primary, secondary and tertiary air fan and also a flue gas fan.

The burner ensures a flow of 0.5 kg/s of sawdust, having a 15500 kJ/kg calculation calorific heat value.

The elemental analysis of the sawdust was:

$$C^i = 44{,}8\%, \quad H^i = 4{,}8\%, \quad O^i = 33{,}2\%,$$

$$S_c^i = 0\%, \quad N^i = 1\%, \quad A^i = 5{,}6\%,$$

$$W_t^i = 10{,}6\%$$

A primary air to the secondary air ratio of 0.5÷ 0.8 is proposed. The excess air ratio at the burner level is imposed in the limits: $\lambda = 1.2 \div 1.25$.

The burner has also a system of swirling blades for each of the air circuits.

The primary air velocity is recommended to be W_1 = 25 – 35 m/s, for the secondary air W_2 = 30 35 m/s, and for the tertiary air W3= 20 – 30 m/s.

An alternative for the axial blades system using one with radial blades is proposed. The swirl ratio used for different jet categories was of 1.2 for the secondary air and of 5.4 for the tertiary air.

3. RESULTS FROM TESTING ON THE UPB PILOT BOILER

The burner presented in figure 1, was mounted on the Politehica University of Bucharest pilot boiler.

The active dimensions of the pilot burner are 1.2 · 1 · 5.9 m. The burner is mounted in the burner embrasure destined to the pulverized solid fuels- figure 2. After the testing, the burner achieved the design thermal power of 600 kW.

The value for the thermal load of the furnace, during the testing, was q_v = 105 kW/m^3, a value which is inside the stability limitations for a furnace burning pulverized solid fuel (thermal load values over 80 *kW/m*^{3} are recommended).

The CO emission was extremely low, under 80 ppm (the layered burning has CO emissions in the 600÷-4000 ppm range).

The 600 kW thermal power of the burner was imposed by the reduced size of the boiler embrasure (∅168). For a larger embrasure, the thermal power of the burner may be increased accordingly. A mention is made that an industrial boiler may have several burners, thus resulting in an increased thermal power. An estimate is made regarding the construction, without major difficulties, of boilers having a thermal power up to 10 MW.

The installation start-up was made by heating using natural gas, cold start using an ignition spark not being recommended by the authors because of the excessive fouling of the heat exchangers.

In the figure 1 a general view of the sawdust burner is presented, in which its self sustaining construction is to be remarked. The

burner is leaned against a side wall of the pilot burner before being mounted.

Figure 1. General view of the pulverized state sawdust burner

Figure 2. The embrasure of the UPB pilot boiler where the suspension sawdust burner was mounted

In figure 2 is presented the constructive part of the burner to be mounted in the furnace embrasure.

The details for the swirling blades are presented in figure 3.

Figure. 3. Detail of the burner construction, pointing out the axial blades for the swirling of the tertiary air.

4. CONCLUSIONS

In order to burn sawdust in suspension a 600 kW thermal power burner was developed. Tests for the energetic performances of the burner were carried out by means of implementing it into a medium power pilot boiler. The experimental results confirmed the technological benefices of burning the sawdust in suspension, leading the way to enlarging the thermal power range of this variant of burners.

REFERENCES

[1] Rădulescu C., Lăzăroiu Gh., Pîşă I., ş.a, 2010 „Researches on the Negative Effects Asseessment (Slugging, Clogging, Ash Deposits) Developed at the Biomass-Coal Co-Firing". Enviromental Engineering and Management, Vol. 9, No.1, January/February 2010, pg. 17-25.

[2] Pîşă I., Rădulescu C., Lăzăroiu Gh., Negreanu G.,ş.a., 2009, „The Evaluation of Corrosive Effects in Co-Firing Process of Biomass and Coal, Environmental Engineering and Management Journal, Vol.8, No.6, November/Decembre 2009, pg. 1485-1490.

[3] Antonescu N., Polizu R., 1988 „*Valorificarea energetică a deşeurilor",* Editura Tehnică, Bucureşti, 352 pag

TRIGENERATIVE PLANT WITH ORGANIC RANKINE CYCLE

Marcel DRAGAN, Tanase PANAIT, Krisztina UZUNEANU, Gelu COMAN

"DUNĂREA DE JOS" UNIVERSITY OF GALAȚI, Romania

Rezumat: Nevoia de protecție a mediului, corelat cu dezvoltarea energetica durabila a condus în ultimii 15-20 de ani la o creştere a preocupărilor legate de promovarea surselor regenerabile de energie şi a tehnologiilor adiacente acestora. Politica Uniunii Europene în această chestiune, exprimată prin cartea albă şi Directiva Europeană 201/77/CE în ceea ce priveşte producția de energie din surse regenerabile precizează că, până în anul 2010, Uniunea Europeană asigură 12% din necesarul de energie prin exploatarea surselor regenerabile. Această lucrare prezintă modul în care se obține energie într-o instalație trigenerativă folosind energia geotermală ca principala sursa. Este prezentat un studiu energetic pepentru o instalație trigenerativă care produce apa caldă, vapori supraincălziți pentru energie electrică şi căldură.
Cuvinte cheie: trigenerare, , ciclul Rankine, pompa de căldură, eficiență termodinamică

Abstract: The need of protecting the environment, correlated with the sustainable energetic development has led in the past 15-20 years to an increase in the concerns regarding the promotion of the regenerating energy sources and their adjacent technologies. The European Union's policy in this matter, expressed by the White paper and the European Directive 201/77/CE regarding the energy production from regenerating sources states that, by the year 2010, the European Union is to assure 12% of its energy requirements from the exploitation of regenerating sources. This work presents how to obtain energy into a trigenerative plant using as main energy source the geothermal energy. An energetic study on the tri-regenerative plant that produces hot water, superheated vapors for electric power and heat is presented.
Keywords: Trigeneration, organic Rankine cycle, heating pump, thermodynamic efficiency

1. INTRODUCTION

Many European countries possessing geothermal resources similar to Romania's have made efforts in designing and applying certain effective and sustainable technologies, leading to a profitable exploration, both in the part regarding the resources' exploitation (geothermal bores extraction and drilling technologies) and in the one regarding the surface energetic devices.
The "low temperature" geothermal resources are used in heating and preparing the domestic hot water of the households, social services, the industrial sector or spaces destined for animal husbandry.

2. GENERAL ASPECTS REGARDING THE GEOTHERMAL ENERGY

The geothermal energy is the heat accumulated in the rocks and the fluids filling their pores. It represents the thermal energy contained by the organic matter underneath the Earth, known as the sensitive heat and greatly produced by the slow decomposing process of the natural radioactive substances existing in all the rock types. The heat comes from the energy diffused radially from the center towards the exterior of the Earth and is produced on a constant basis. The high temperatures of the center of the Earth can be explained by the Earth's origin and the existence of the uranium (U^{238}, U^{235}), thorium (Th^{232}) and potassium (K^{40}) radioactive isotopes in its composition.
The diffusion process is permanent and it could be stated that the geothermal energy is an inexhaustible energy source.
The geothermal energy is one of the alternatives able to cover mankind's need of energy, also minimizing the impact on the environment.

2.1 The geothermal gradient

The geothermal gradient expresses the depth induced temperature increase, the average being of de 2,5…3°C/100 m, corresponding to an 100 °C temperature, at 3000 m in depth.
There are various zones where the geothermal gradient's value considerably varies from the aforementioned average. For example, in the areas where the rock plateau has experienced sudden collapses and the reservoir is filled with "very young" sediments (from the geological point of view), the geothermal gradient may be less than 1°C/100 m. On the other hand, in other geothermal areas, the gradient can surpass the average by several times. In general, the gradient's value is of

25 ^{0}C/km, however there are numerous areas where These precise areas are true high potential geothermal energy underground reservoirs, which, in certain favorable conditions, may be explored in order to be used for the heating equipments preparing the domestic hot water.

2.2. Geothermal systems

The geothermal systems can be found in areas with a normal or near normal geothermal gradient and in the areas where the geothermal gradient may be slightly above average. In the first situation, the systems will be characterized by low temperatures, usually reaching 100°C for economically optimal depths. In the second case, the temperature may even reach 400°C. A geothermal system may be described as one where water is used as a heat transport agent, through which the heat is taken from the underground source to the consumer at surface. A geothermal system is made up of three main elements: a heath source, a reservoir and a fluid. The source may be a magmatic rock intrusion of a very high temperature (> 600°C), located rather near the surface (5-10 km). The reservoir is a hot, permeable rock volume, where the transporting fluids extract the heat from.

The reservoir is usually covered by an impervious rock layer, connected to a surface charging area through which the geothermal fluid originating in the precipitation may partially or entirely compensate for the loss in the reservoir through springs or the extraction process. The geothermal systems may be classified depending on the temperature and pressure of the system, as well as the way the thermal energy is transferred to the soil. Consequently, there are several geothermal systems, listed as follows:

a. Hydro-thermal sources

These sources are based on the circulation of meteoric (surface) waters, which infiltrate from 100 m to 4,5 km into the Earth's crust.The circulation is naturally assured by the difference in the density of the cold and hot water, or of the water vapors.

b. Pressured sources

The water contained in the reservoirs has a low salt concentration and contains dissolved methane. The water and methane are held captive by impervious rock layers in reservoirs at great depths (3-6 km), characterized by extremely high pressure levels. The water's temperature is generally between 90 … 200 °C.

c. Hot rocks

This source type is based on hot rock layers existing on the Earth's crust. Unlike the hydro-thermal sources, in this case there are no underground water reservoirs, nor is there any possibility for the meteoric water to infiltrate.The exploration is carried out through drilling in the hot rocks area. Cold water will be pumped in order to create a reservoir, and the water heated this way will eventually be brought back to the surface through an extraction shaft.

d. Magma

The magma is the greatest geothermal resource, being formed of melted rocks, located at great depths of 3 to 10 km. The magma's temperature is generally situated between 700 and 1200°C. No research has been carried put regarding the use of this resource, due to the difficult access at the depths the magma can be found.

3. SOLUTION FOR TRIGENERATION OF A GEOTHERMAL SOURCE

The great majority of the geothermal reservoirs are characterized by relatively low temperatures, ranging from 100 .. 200°C. In this case, for the conversion of the geothermal energy into electricity and thermal energy, the optimal solution is using the plant from Fig. 1.

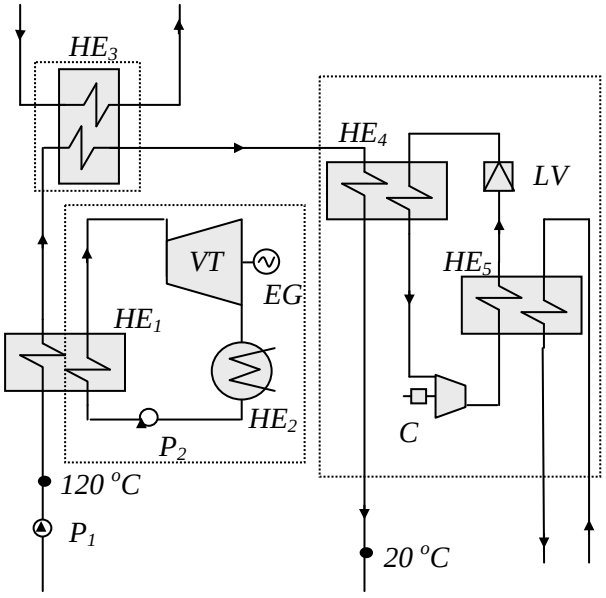

Fig 1. *Trigeneration plant*

The water from the geothermal source, with a temperature of 120 ^{o}C, gives in to the refrigerant agent of the Rankine Cycle (amonia), the heat. The main characteristic of this fluid is the much lower boiling point than water. The vapors formed into the vaporizer HE1 will expands in the vapor turbine VT and will produce electric energy in the electric generator

The water cooled condenser HE2 forms the liquid refrigerant agent, which is pumped out with pump P2, and reintroduced into the vaporizer HE1.

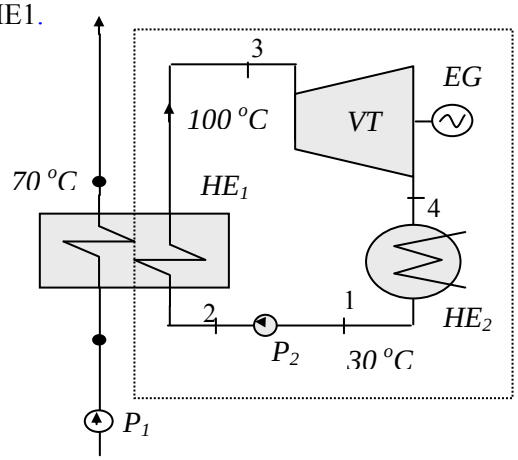

Fig 2. *Electric plant with ammonia Rankine cycle*

The hot water is produced by cooling out the geothermal water, from 70 °C to 40 °C in the heat exchanger HE3.

The water for use is heated from 15 °C to 55 °C.

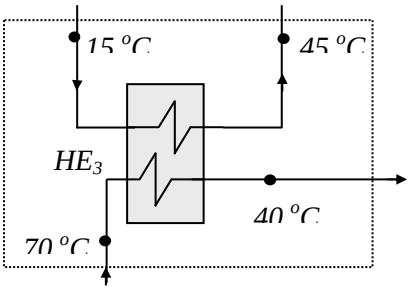

Fig 3. *The generation of hot water for use*

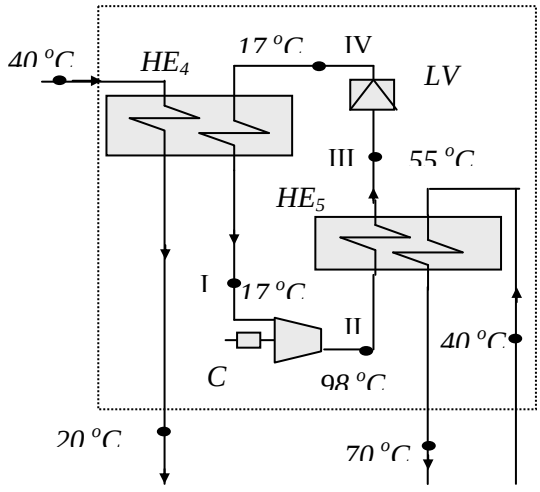

Fig 4. *Producing heat with the heat pump*

The low thermal potential of geothermal water with a temperature below 40 °C is used with an ammonia heat pump installation. Cooling out the geothermal water in the heat exchanger HE4, the ammonia is vaporized at 17 °C. Those refrigerant vapors are compressed in the compressor C and condensate in the condenser HE5. Condensing the ammonia gives in the condensing heat to the water from the heating cycle, generating a useful effect.

The liquid ammonia expands in the laminar valve LV. For the compressor from the heat pump installation the electric energy produced in the Rankine cycle is used.

4. THE TRIGENERATIVE PLANT ENERGETIC ANALYSES

The energetic analysis of the geothermal energy conversion in to useful energy is made on the three selected perimeters.

*In the Rankine cycle with ammonia are the following energy flows (according to fig. 2),

$$q_{0,1} = c_w(120-70)\,[kJ/kg] \quad (1)$$

$$l_p = v_1(p_2 - p_1)\,[kJ/kg] \quad (2)$$

The work produced by the turbine:

$$l_{VT} = h_3 - h_4\ [kJ/kg] \quad (3)$$

The thermal efficiency of the Rankine cycle is,

$$\eta_t = \frac{l_{VT} - l_p}{h_3 - h_2} \quad (4)$$

The specific energy provided by the installation is:

$$ee = \eta_{gen}(l_{VT} - l_p)\,[kJ/kg] \quad (5)$$

η_{gen} =0.8, represents the turbo generator efficiency

* for the thermal energy used to warm up the water for use in the heat exchanger HE3, the specific energy consumed is:(according to fig. 3):

$$q_{0,2} = c_w(70-40)\,[kJ/kg] \quad (6)$$

Supposing that the heat exchanger is adiabatic insulated, the produced energy is:

$$q_{h,w} = q_{0,2} = c_w(70-40)\,[kJ/kg] \quad (7)$$

***** For the thermal energy for heat, according with the heat pump installation from fig. 4 the following energy is used:

- for the refrigerant vaporize

$$q_{0,3} = c_w(40-20)\,[kJ/kg] \quad (8)$$

- for the refrigerant compressor drive

$$l_c = h_{II} - h_I\ [kJ/kg] \quad (9)$$

The condensation energy generated by the heat exchanger (condenser) HE5:

$$q_h = h_{II} - h_{III}\,[kJ/kg] \quad (10)$$

*the energetic efficiency of the trigenerative plant is mathematically expressed with the relation (11):

$$\eta_{trigen} = \frac{(ee - l_c) + q_{hw} + q_k}{q_{0,1} + q_{0,2} + q_{0,3}} \quad (11)$$

4.1. The energy studies result

* from ammonia Rankine cycle, the thermodynamic parameters of the main characteristic points are:

Table 1. Numerical results

Point	*t [°C]*	*p [bar]*	*i [kJ/kgK]*	*x [kg/kg]*
1	*30*	*11,67*	*-620,6*	*0*
2	*31,4*	*62.53*	*-612,14*	*-*
3	*100*	*62.53*	*473*	*1*
4	*30*	*11,67*	*291,24*	*0,79*

The thermal efficiency of the ammonia Rankine cycle (equations 4) is 16 %.
The plant generates the following specific energy (equations 4):
ee=138,64 kJ/kg.

* from heating pump cycle, the thermodynamic parameters of the main characteristic points are:

Table 2. Numerical results

Point	*t [°C]*	*p [bar]*	*i [kJ/kgK]*	*x [kg/kg]*
I	*17*	*7,78*	*514,78*	*1*
II	*98*	*23,09*	*671,1*	*-*
III	*55*	*23,09*	*-496,12*	*0*
IV	*17*	*7,78*	*-496,12*	*0,156*

For the drive of the refrigerant compressor from the installation with heating pump, according to equatio(9), the following specific energy is consumed: $l_c = 156,32\ kJ/kg$

We will observe that the specific work necessary for the compression in the heat pump installation is bigger than the specific electric energy obtained in the Rankine cycle. In these conditions for the installation to work properly is necessary that between the required electric power for the heat pump installation and the electric power produced by the energetic installation with ammonia, to exist the relation:

$$P_{EE} = m_{Rankine} \cdot ee \geq P_c = m_{hp} \cdot l_c\ [kJ/kg] \quad (12)$$

Therefore the function terms are connected to the relation between the two flows:

$$m_{Rankine} \geq 1,282 \cdot m_{hp}$$

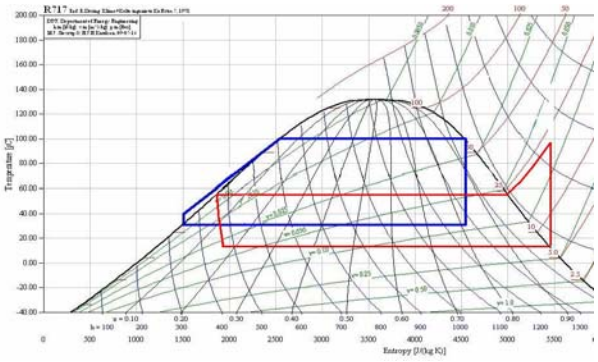

Fig 5. *Ammonia Rankine cycle and ammonia heating pump cycle*

The trigenerative plant in the limit function situation will become a cogenerative plant with the following efficiency:

$$\eta_{cogen} = \frac{q_{hw} + q_k}{q_{0,1} + q_{0,2} + q_{0,3}} \quad (13)$$

$$\eta_{trigen} \geq \eta_{cogen} = 0,6$$

5. CONCLUSIONS

Using the geothermal energy in trigenerations, in order to produce electricity and thermal energy has certain advantages, among which:
*The thermal efficiency compared with the efficiency of the Rankine cycle of the nuclear plants;
*It is a local primary energy source able to reduce the importation of expensive fossil fuels (natural gas, petroleum);
*It has a positive impact on the environment by replacing certain extremely polluting fossil fuels (charcoal); it represents a reliable primary energy source, not needing any storing equipment.

REFERENCES

[1] Dubin F.S. *The heat pump centered integrated Community energy system* ASHRAE, 1999, vol.86, p.979-990.
[2] *Geothermal Energy. Resources, Production, Stimulation,* Stanford University Press, 2002.
[3] Hickel W.T.**,** *Geothermal energy, A special report,* University of Alaska, Fairbanks, 2002.

MANAGEMENT FOR ENERGETICAL PURPOSES OF THE RECOVERING ENERGETICAL RESOURCES WITH LOW THERMAL POTENTIAL

Valeria Miron

Universitatea „Dunarea de Jos" din Galati, Romania

Rezumat. Această lucrare prezintă modelul termodinamic de calcul, bazat pe ecuatiile de conservare a energiei, masei pe component si masei totale, pentru instalația friforifică cu resorbție. Sunt prezentate, de asemenea, modalitățile de recuperare a energiilor disponibile din procesele industriale.
Cuvinte cheie. Instalație frigorifică cu resorbție.

Abstract. The paper presents the one of the modernizing methods for the management of the fuel and energy in the industrial fields. The presented method it is based on the resorbtion refrigeration system. These system use directly the industrial recoverable energetically saving though considerable of fuel and electric energy.
Keyword. Resorbtion refrigeration plant.

1. INTRODUCTION

On of the modernizing methods for the management of the fuel energy in the industrial field is using the recoverable energetically resourses (RER) from the tehnological proceses into the tehnological proces itself and if possible outside it, for energically purposes such ast producing hot-water, heating, air conditioning, refrigeration etc.

For tehnological refrigeration or for confort tehnological air conditioning the refrigeration plants with vapor compression, whitch generally use electrical energy, can be replaced with resorbtion refrigerating systems. These systems use directly the industrial RER saving though considerable quantity of fuel and electric energy.

The resorbtion refrigerating systems functioning assume:

- the existence on its netghborhood of a heating source with low potential (RER) and of a cooling user;
- the energetic potential of the RER to be bigger than the neede for the cooling production;
- the simultaneously existence of the heating source and the cooling user.

refrigeration systems;

2. R.E.R. WITH LOW THERMAL POTENRIAL

The resorbtion refrigeration system was designed built and analyzed in terms of using the steam as heating agent for vapor-generator.

As an industrial RER the steam can the useful like secondary steam and exhaust steam.

Exhaus steam

Sourse from power machines which use the steam for their driving (forging machines, deep-drawing machines, presses), pumps, compressor etc.

Using area heating, ventilation, air conditioning, hot-water supply of the industrial workshops, administrative buildings and industrial cooling production in absorbtion-resorbtion systems by using directly the exhaust steam in the vapor-generator.

The recovering functional schemes can be:

- with direct supply (fig.1) for heating, ventilation, hot-water production, for in adsorbtion-resorbtion refrigeration systems;
- with indirect (fig.2) for heating, ventilation, hot-water production, for in adsorbtion-resorbtion

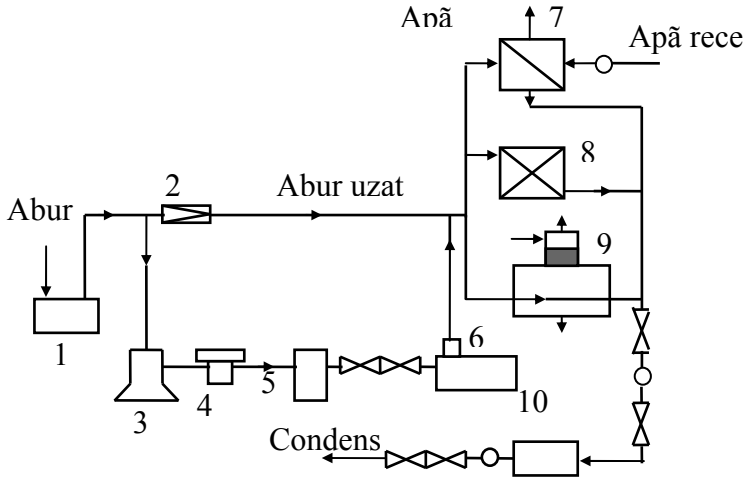

1 – steam collector; 2 – throttle valve; 3 – power machine; 4 – filtre; 5 – oil trap; 6 – exhaust steam collector; 7 –recuperative heatexhantor; 8 – consumer; 9 – vapor generator of the refrigeration plant; 10 – condensator collector

Fig.1.

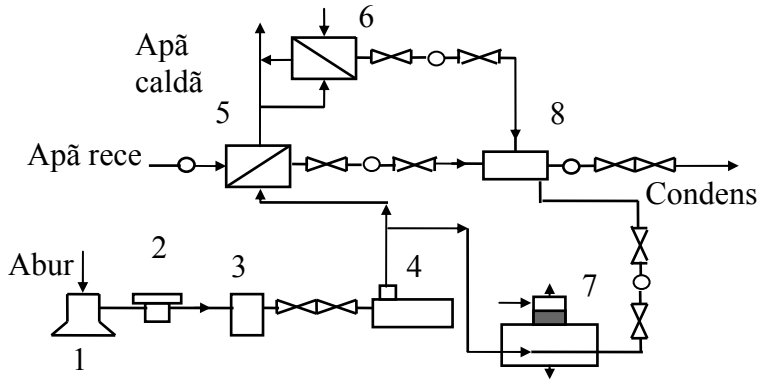

1 – power machine; 2 – filter; 3 – dil trap; 4 – exhaust steam collector; 5 – recuperative heat exhanger; 6 – peak preheater steam-water; 7 – vapor generator of the refrigeration plant; 8 – condensate collector

Fig.2.

The preheater 4 warm up the to 80...90^{o}C using exhaus steam at 1,3...1,5 bar, and proheater 6 warm up the water to 130...140^{o}C usine life steam. The advantage of this scheme consist in total collectimg of the condensate from the exhaust steam.

Using the exhaust steam for the industrial cooling production in refrigeration systems with resorbtion in industrial area where cooling is needed in summertime and heating on wintertime assure the increase of the annual functioning period of the recorvering of the exhaus steam.

The exhaus steam can be wet saturated steam or overheated steam, at relativels low pressure 1,1...2,5 bar. For the power machines the steam flow depends on falling mass having sudden variation (from 0 to 100%). For pumps, compressors and blowers the steam flow has continnous shape with variation in function of the process and of the control method. In order to get uniform flow variations the exhaus steam collector 4 can be used.

Heat savings.

For the exhaust steam got from the power nachines the recovered heat Q_{rer} , can be calculated with the relation:

$$Q = D \cdot \Delta h \text{ [kW]} ,$$

wrere: D – exhaust steam flow [kg/s]

Δh – steam enthalpy variation [kJ/kg].

Secundary steam

Sorce: from steam generator purge.

Using area: supply water preheating of the boiler heating, ventilation, consumption hor-water production, industrial cooling production in absorbtion-resorbtion systems by using directly the exhaust steam in the vapor-generato.

Using restriction:

The secundary steam resulted from technological processes has a high pressure it doesnt contain oil marks, but can contain chemical residues.

For saturated secundary steam the recovered heat can be calculated with:

$$Q_{rer} = D \cdot r \text{ [kW]} ,$$

where: D – secundary steam mass flow [kg/s]
r – latent heat of condensation [kJ/kg]

3. RESORBTION REFRIGERATION PLANT

A resorbtion refrigerating system (fig.3) is made by two vapor-generator, GV and Deg, two adsorbers, Ab and Res, two heat exchangers (economizer), EC1 and EC2 and two solution circulation pumps, P1 and P2. This configuration makes the instalation more voluminous and more complicated in comparation with the simple absorbtion refrigerating system. The main advantage of the resorbtion refrigerating system is the fact that the pressures p_o and p_F from the low-pressure, respectively, high pressure part of the system, are no longer determined by the vaporizing temperature t_o, and the condensing temperature t_k, as they are on the absorbtion refrigerating system. The vapor absorbtion processes in the resorber and the vapor producing process in the degasser can take place at any pressure values, being independent of the temperature. The pressures p_o and p_F can be choused randomly, especially closer t_o the atmospheric pressure value. This, problems like tightening, dimensioning, pump construction are simplified and the thermal potential of the heating agent in the vapor generator can be reduced making possible the use of the RER with a lower thermal potential than one used on absorbtion refrigerating systems.

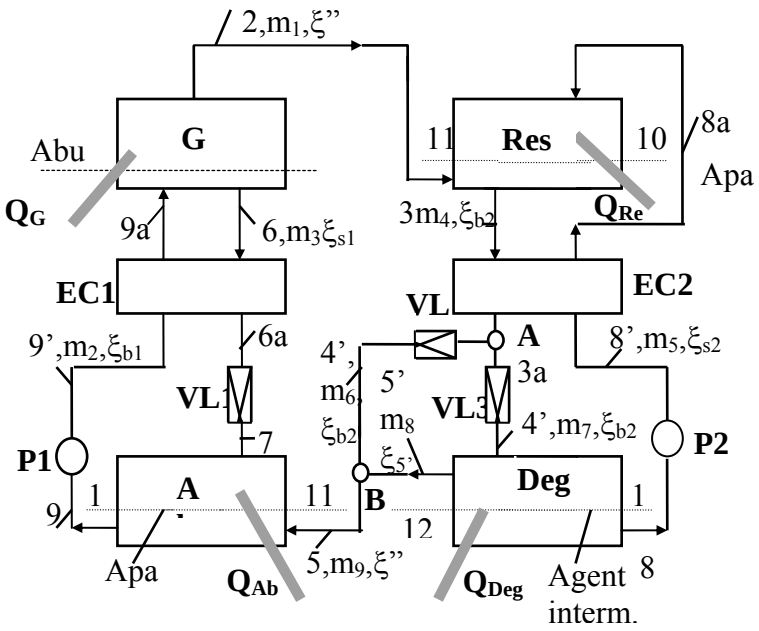

Fig.3. *The resorbtion refrigeration functional scheme*

4. THERMODYNAMIC MODELING

The resorbtion refrigeration modeling is based on energy conservation equations and the mass conservation equations for resorbtion refrigeration are:

- equation of energetic inventory on the Degasser:

$$\dot{m}_8 \cdot \left(h_4 - h_8\right) \cdot \frac{\xi_{b2} - \xi_{5'}}{\xi_{b2} - \xi_{s2}} + h_{5'} - h_4 = \dot{Q}_0$$

- equation of material inventory on the Degasser:

$$\dot{m}_5 = \dot{m}_8 \cdot \frac{\xi_{5'} - \xi_{b2}}{\xi_{b2} - \xi_{s2}}$$

- equation of mass inventory on the Degasser:

$$\dot{m}_7 = \dot{m}_5 + \dot{m}_8$$

- equation of energetic inventory on the Absorber:

$$\dot{Q}_{Ab} = \dot{m}_9 \cdot h_5 + \dot{m}_3 \cdot h_7 - \dot{m}_2 \cdot h_9$$

- equation of material inventory on the Absorber:

$$\dot{m}_3 = \dot{m}_9 \cdot \frac{\xi'' - \xi_{b1}}{\xi_{b1} - \xi_{s1}}$$

- equation of mass inventory on the Absorber:

$$\dot{m}_2 = \dot{m}_3 + \dot{m}_9$$

- equation of energetic inventory on the economizer EC1:

$$m_3 (h_6 - h_{6a}) = m_2 (h_{9a} - h_9$$

- equation of energetic inventory on the Vapor Generator GV:

$$\dot{Q}_{GV} = \dot{m}_1 \cdot h_2 + \dot{m}_3 \cdot h_6 - \dot{m}_2 \cdot h_{9a}$$

- equation of material inventory on the GV:

$$m_1 \xi\text{“} + m_3 \xi_{s1} = m_2 \xi_{b1}$$

- equation of mass inventory on the GV:

$$m_1 + m_3 = m_2$$

- equation of energetic inventory on the Resorber:

$$\dot{Q}_{Res} = \dot{m}_4 \cdot h_3 + \dot{m}_1 \cdot h_2 + \dot{m}_5 \cdot h_{8a}$$

- equation of material inventory on the Resorber:

$$\dot{m}_1 = \dot{m}_5 \cdot \frac{\xi_{b2} - \xi_{s2}}{\xi'' - \xi_{b2}}$$

- equation of mass inventory on the Resorber:

$$\dot{m}_4 = \dot{m}_5 + \dot{m}_1$$

- equation of energetic inventory on the economizer EC2:

$$m_4 (h_3 - h_{3a}) = m_5 (h_{8a} - h_8)$$

- equation of material inventory on the nod A:

$$\dot{m}_6 = \dot{m}_4 - \dot{m}_7$$

- equation of material inventory on the nod B:

$$\dot{m}_9 = \dot{m}_8 + \dot{m}_6$$

The problem is determined because the number of the equations is equal with the number of the unknowns: m_1, m_2, m_3, m_4, m_5, m_6, m_7, m_8, m_9, ξ_5, h_{6a}, h_{8a}, Q_F, Q_{Ab} and Q_{Res+}.

After calculation, we get $m_1 = m_2$ and $\xi_5 = \xi''$, which are essential conditions for continuous functioning of the resorbtion refrigerating system.

The performance coefficient of the system is:

$$COP = \frac{Q_o}{Q_{GV}}$$

The energetic efficiency, η_{ex}, is au important criteria of performance evaluation of the resorbtion refrigerating sustem, because the energies are taken into consideration by the quantity and also by their quality point of view:

$$\eta_{ex} = \frac{E_{Q_o}}{E_{Q_{GV}}} = \frac{Q_o}{Q_{GV}} \cdot \frac{T_a - T_{om}}{T_{Fm} - T_a} \cdot \frac{T_{Fm}}{T_{om}}$$

Where:

T_{om} – the average boiling temperature of the solution in the degasser zone:

$$T_{om} = 0,5 \, . \, (T_{omi} + T_{oma}) \, [K]$$

T_{Fm} – the average boiling temperature of the solution in the vapour generator:

$$T_{Fm} = 0,5 \, . \, (T_1 + T_6) \, [K]$$

The resorbtion refrigerating system calculation was made under the following condition:

- the refrigeration power of the system $Q_o = Q_{deg} = 100$ w;
- the minimal boiling temperature of the hydroammonia solution in the degasser $t_{o,min} = -10^oC$;
- the initial temperature of the absorber and resorber cooling water $t_{wr} = 20^oC$;

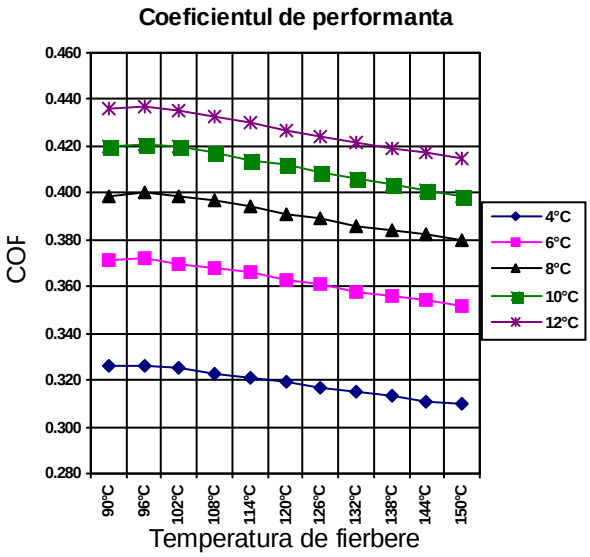

Fig.4. *COP in function of the boiling temperature and the degassing zone: t_k = 30°C; t_o = -10°C; p_F = 9 ata; Q_o = 100 kW*

- the hydroammonia solution temperature at the absorber, respectively resorber exit $t_9 = t_3 = 30^oC$.

As variable parameters were considered:

- the heating agent temperature in the vapor generator (RER), respectively the maximum boiling temperature of the hydroammonia solution $t_F = t_6 = 90...150^oC$;
- the boiling pressure of the hydroammonia solution p_F = 8, 9 and 10 ata, on the condition p_F , p_k;
- the degassing zone $\Delta\xi$, determined by the temperature variation in the degasser, Δt_D = 4...12°C.

In order to make calculation, it was used a set of equations that describe the thermodynamic model of the H_2O – NH_3 binary mixture. These equations were integrated in oroginal softwarw. The advantage of using this model is given by the high evaluation accuracy of the state points, comparingwith the using of the common method with the h – ξ diagram, were the reading accuracy of the values is relative.

The calculation were made for p_F = 9 ata, taking into consideration that the heatimg agent temperature of the vapor generator is more important than the maximum wpok temperature in the refrigeratong system.

The rezult obtained for each variant of calculation previously mentioned allowed the underlinding of the tendencies of the proportions calculated after modifying some parameters considered as variable.

For the performance evaluation of the resorbtion refrigerating system are presented performance coefficient, COP (fig.4). Depending on the boiling temperature, the perfoermance coefficient present a maximum around the value of 96°C after which it uniformly decreases.

CONCLUSIONS

This paper presented an adaptation of the resorbtion refrigerating installation following the thermodinamic model of the resorbtion refrigerating cycle and thermodinamic model of the H_2O – NH_3 binary mixture for the purpose of improving it at the desing level. The adaptation effort has been justifiable since we managed to influence the main proportions according to the desing parameters currently used when calculating these types of refrigerating installtion. In addition, there have been identified a minimum number of „requirements" for the refrigerating cycle in order for this to be able to work within the designed parameters and with acceptable values for the performance coefficient. The thermodynamic model of the H_2O – NH_3 binary mixture, once completed, allows the studying of different types of resorbtion thermodynamic cycles with the purpose of improving their efficiency.

REFERENCES

[1.] Gheorghiu,C., *Contributii la studiul proceselor de transfer de cãldurã si masã în generatorul de vapori al instalatiei frigorifice cu absorbtie*, Teza de doctorat, IPB, 1982.

[2.] Grossman,G., Wilk,M., *Advanced modular simulation of absorption systems*, Rev.Int. du Froid, 1994, Volume 17, Numero 4, pg.231-244.

[3.] Grossman,G. *Modular and flexible simulation of advenced absorption systems, Proceedings of the International Absorption Heat pumps*, Conference ASME, 1993, pg.345-351.

[4.] I.I.R., *Thermodynamic and physical properties NH_3-H_2O*, 1994.

[5.] Maczek,K., *Optimization in Design of Absorbtion Refrigeration Systems*, I.I.R.

[6.] Commissions B1, B2, C2, D1, D2/3, Wageningen, 1988.
[7.] Miron,V., Cercetãri experimentale privind utilizarea resurselor termoenergetice de potential scãzut în producerea frigului cu ajutorul instalatiei cu resorbtie, Teza de doctorat, Universitatea din Galati, 1999.
[8.] Porneala ,S., *Unele consideratii asupra instalatiei frigorifice cu resorbtie*, Rev.de Chimie 33, nr.8, 1982.
[9.] Schulz,S., *Equations of state for system ammonia-water for use with computers*, Proc.XIIIth Int.Cong.Refrig., Washington, 1971.
[10.] Vilcu,R., *Termodinamica chimica*, Ed.Tehnica, Bucuresti, 1994.
[11.] *** ASHRAE Handbook, Fundamentals, 1987

THE ENERGETICS AND THE STOICHIOMETRIC COMBUSTION EQUATIONS

Nicusor Vatachi, Spiru Paraschiv, Ion C. Ionita

"Dunărea de Jos" University of Galați, Romania
E-mail: nvatachi@ugal.ro

Rezumat In lucrare este discutata utilizarea in energetica a ecuatiilor stoechiometrice in calculul arderii combustibililor organici. Plecand de la ecuatiile stoechiometrice de ardere scrise pentru carbon, hidrogen, sulf si combustibili gazosi, autorii arata ca aceste ecuatii se bazeaza numai pe legea conservarii masei, fara sa tina cont de legea conservarii energiei, exprimata prin ecuatia relativitatii restranse formulata de Albert Einstein. Pentru calculele cantitative ingineresti ecuatiile stoechiometrice ale chimiei sunt destul de precise, dar pentru a pune in evidenta scopul principal al energeticii, obtinerea de energie, ecuatiile de ardere trebuie scrise respectand legea conservarii combinate a masei si energiei. In lucrare autorii propun utilizarea unor forme mai complete si corecte pentru ecuatiile de ardere, forme care includ si evidentiaza obtinerea de energie prin consum de masa, conform teoriei relativitatii restranse.
Cuvinte cheie:calculul arderii, ecuatii stoechiometrice, teoria relativitatii reatranse-Einstein.

Abstract *The paper is discussing the use of stoichiometric combustion equations in energetics, namely in the fuel burning calculus. Starting from the combustion stoichiometric equations written for carbon, hydrogen, sulphur and gaseous fuels, the authors show that these equations are based only on the mass conservation law, not taking into consideration the energy conservation law, expressed by Albert Einstein's equation of relativity theory. For engineering calculus, the stoichiometry combustion equations are enough precise, but in order to put in evidence the main goal of energetics, that is the energy production, the combustion equations must be written taking into consideration both the mass and the energy conservation laws. They propose the use of a more complete and correct form of combustion equations, which include the energy obtaining.*

Key words*: combustion calculus, stoichiometric equations, Einstein's restricted relativity theory.*

1. THE PURPOSE OF THE PAPER

The paper is dealing with Albert Einstein's theory of relativity applied to organic fuels combustion. We consider that today, when the scientific word is no longer satisfied with the value of 300,000 m/s for light speed, as it was considered by Einstein and it is corrected to 299,792,458 m/s, that is with o relative difference of 0,06918 %, we must not be satisfied with stoichiometric combustion equations, based only on the mass conservation principle.

More than one century ago, Albert Einstein formulated in 1905 his restricted relativity theory, expressed by the well known but maybe not entirely understood equation E=mc2. One of the effects we signalize today in the paper is the mass reduction while energy is delivered during the exothermal process of the combustion of organic fuels.

Which is the mass reduction while one kilogram of organic fuel is burnt, how much is it representing percentage? How big is it the error we are making when we are neglecting this reduction in the stoichiometric calculus of the combustion? These are the questions aroused and answered in the paper.

2. THE TODAY SITUATION

Let's remember that stoichiometry is a branch of chemistry that deals with the relative quantities of reactants and products in chemical reactions [11].

In the paper [2] and in the majority of the others of specialty [6-10], the combustion of the carbon is expressed by the well known stoichiometric equation

12 kg C + 32 kg O2 $\rightarrow$ 44 kg CO2 (1)

The arrow used instead of the equal sign shows that is a chemical reaction, although the amount of kilograms is kept, according to mass conservation law, respected in stoichiometry.

The paper [5] advances one step and writes:

12 kg C + 32 kg O2 $\rightarrow$ 44 kg CO2 $\oplus$ 406,45 MJ (2)

showing this way the purpose of the fuels burning, that is the delivering of the 406.45 MJ/kmol. In the paper it is specified; "In order not to make dimensional calculus mistakes it was used the sign $\oplus$, which expresses a delivered heat, due to exothermic process ". Let's remark that the equation [2] is not dimensional, because one could not add mass measure units [kg] with energy measure units [MJ]. Also, in this equation it was not possible to use the equal sign between the entering and the exiting amounts of the combustion process.

3. WHAT IT IS PROPOSED

Let's advance one step using Einstein's equation $E = m \cdot c^2$ and let's write that the energy variation ΔE (fig.1) achieved by the out side heat of the combustion process have provoked the mass reduction Δm, that is

$$\Delta E = c^2 \cdot \Delta m \quad (3)$$

As result, the mass reduction we want to express is the following

$$\Delta m = \Delta E / c^2 \quad (4)$$

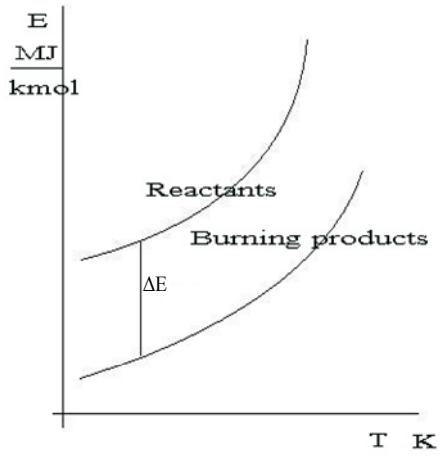

Fig.1 The energy variation ΔE

We will use the same way to describe the combustion of the other components or fuels.

For the incomplete combustion of the carbon:

1 kmol C + 0,5 kmol O2 = 1 kmol CO + $\Delta E_{C_i} / c^2$ (6)

For hydrogen burning:

1 kmol H2 + 0,5 kmol O2 = 1 kmol H2O + $\Delta E_{H_i} / c^2$ (7)

For sulphur burning:

1 kmol S + 1 kmol O2 = 1 kmol SO2 + $\Delta E_S / c^2$ (8)

For carbon monoxide burning:

1 kmol CO + 0,5 kmol O2 = 1 kmol CO2 + $\Delta E_{CO} / c^2$ (9)

For methane burning:

1 kmol CH4 + 2 kmol O2 = 1 kmol CO2 + 2 kmol H2O + $\Delta E_{CH_4} / c^2$ (10)

For the next calculations we used the table 1, in which we wrote enthalpies of formation ΔE for the above mentioned components or substances, and the mass reductions $\Delta E / c^2$ for each of them.

Table 1. Calculation of relative errors ε r

No.	The component or the substance	ΔE MJ/kmol	Δ E / c2 kmol	ε r %
1	Carbon (complete burning)	406,45	4,516 x 10^{-15}	5,48.10^{-17}
2	Carbon (incomplete burning)	123,859	1,376 x 10^{-15}	8,73.10^{-17}
3	Hydrogen	286,44	3,18 x 10^{-15}	6,82.10^{-17}
4	Sulphur	296,38	3,29 x 10^{-15}	6,71.10^{-17}
5	Carbon monoxide	110,541	1,376 x 10^{-15}	8,78.10^{-17}
6	Methane	888,172	9,86 x 10^{-15}	1,4.10^{-16}

By examining the results obtained in the last two columns of the table 1 we remark that the relative error ε r committed when using the stoichiometric equations (of equation (1) type) is so small that the mass reduction Δ m could not be measured by today technical means.

4. CONCLUSIONS

4.1. Due to insignificant mass reduction when burning organic fuels, the use of the chemistry stoichiometric equations is quantitatively justified (tab.1).

4.2. The chemistry stoichiometric equations are using only the mass conservation law, without describing the out or in side heat of the chemical reaction processes. But in the case of

organic fuels burning, when the purpose is the heat obtaining, we must use in the combined way the both mass and energy conservation laws. The present paper proposes the use of the equations of (5) - (10) type, where is highlighted mathematically the mass reduction according to Albert Einstein's restricted relativity theory.

4.3. Comparing with equation (2) the equations (5) - (10) are more precise, that is they are dimensional correct, because they use at all the terms the same mass measure unit and more, they are highlighting the purpose of the fuels burning, namely the thermal energy obtaining.

4.4. The insignificant mass reduction Δm when we are burning organic fuels shows how little amount we are extracting by combustion from the kilogram or the kilo mol of fuel and how huge are the energy resources unused yet but waiting to be discovered.

Nomenclature

ΔE [MJ / kmol] - the energy release due exothermic burning process;

Δm [kmol] – the mass reduction while organic fuels are burnt;

c – the vacuum light speed, considered c = 3.108 m/s in this paper;

ΔE_C [MJ / kmol] – the energy release by complete carbon C burning;

ΔE_{C_i} [MJ / kmol] – the energy release by incomplete carbon C burning;

ΔE_{H_2} [MJ / kmol] – the energy release by hydrogen H2 burning;

ΔE_S [MJ / kmol] – the energy release by sulphur S burning;

ΔE_{CO} [MJ / kmol] – the energy release by carbon monoxide CO burning;

ΔE_{CH_4} [MJ / kmol] – the energy release by methane CH4 burning ;

ε_r [%] - the relative error ε_r committed when using the stoichiometric equations;

$\Delta E / c^2$ [kmol] - the mass reduction while organic fuels are burnt (Δm) ;

REFERENCES

[1] Bernard Haisch, Alfonso Rueda & H.E. Puthoff Beyond E=mc2 A first glimpse of a postmodern physics, in which mass, inertia and gravity arise from underlying electromagnetic processes. Published in THE SCIENCES, Vol. 34, No. 6, November / December 1994, pp. 26-31, New York Academy of Sciences.

[2] Russel&Adebiyi - Classical Thermodynamics, Saunders College Publishing, New York, Montreal, London, Sidney, Tokyo,. ISBN 0-03-032417-3.

[3] Tudose Cosma – Fizica atomica si nucleara, Editura Didactica si Pedagogica, Bucuresti.

[4] Tudose C. s.a. – Fizica, Editura Didactica si Pedagogica, Bucuresti.

[5] Ionita C.I. – Generatoare de abur, vol.1, Universitatea Dunarea de Jos Galati.

[6] Stephen R. Turns, An Introduction to Combustion: Concepts and Applications, 2nd Edition, McGraw-Hill Science, 2000.

[7] Panoiu N. Cazane de abur, Editura Didactica si Pedagogica, Bucuresti.

[8] Mihaescu L. s.a. Cazane de abur si apa fierbinte, Editura Perfect in colaborare cu Editura Printech.

[9] Neaga C. s.a. Indrumar.Calculul termic al generatoarelor de abur. Editura Tehnica, Bucuresti.

[10] Moran M.a.o. Fundamentals of Engineering Thermodynamics. John Wiley and Sons Inc. New York,Chichester, Singapore, Toronto.

[11] http://en.wikipedia.org/wiki/Stoichiometry

[12] I.V. Ion, N. Vatachi, I. C. Ionita. Teoria relativitatii si arderea combustibililor organici . ETCNEUR, Bucuresti 2011.

FREEZING METHOD FOR RASPBERRIES AND BLUEBERRIES USING LIQUID NITROGEN

Valeriu DAMIAN [+]***, Cristian IOSIFESCU*** [+]***, Gelu COMAN*** [+]
[+] "DUNĂREA DE JOS" UNIVERSITY OF GALAȚI, Romania.

Rezumat. Metoda prezentată foloseşte pentru congelare azot lichid, care are avantajul costului redus, fiind obținut ca produs secundar în urma procesului de separare a aerului. Lucrarea prezintă aspecte legate de congelarea criogenică cu azot lichid a fructelor de pădure (zmeură şi afine): durata procesului, influența a diferiți parametri, avantajele şi dezavantajele metodei. Congelarea rapidă constă în folosirea într-un congelator criogenic atât a căldurii latente de vaporizare a azotului lichid, cât şi a căldurii specifice a vaporilor de azot formați, a căror temperatură creşte până la temperatura finală a produsului congelat.
Cuvinte cheie: congelare criogenică, fructe de pădure, conservarea alimentelor.

Abstract. Considering the demands for reduction of fuel consumption involved in generation of electrical energy needed for classical refrigeration systems, this method uses for freezing liquid nitrogen obtained as secondary product at oxygen production. The resulted nitrogen gas is discharged in the environment, and, being chemically inert, it does not contribute to generation of harmful chemical components. This paper presents some aspects concerning raspberries and blueberries freezing using liquid nitrogen: duration of the process, influence of various parameters, advantages and disadvantages of this modern method. Quick freezing of food products in a cryogenic freezer consist in the use latent heat of evaporation of the liquid nitrogen, as well as of the sensible heat of the vapors, whose temperature increase up to final temperature of the frozen product.
Key words: berries, freezing, food preservation, nitrogen.

1. INTRODUCTION

Freezing is the favorite modern mean for best preservation of nutrient and organoleptical properties of a large number of alimentary products, ensuring long term preservation. Direct contact freezing using liquids (nitrogen or CO_2), is done either by sinking the product in a cold liquid or by spraying the product with this liquid. Nitrogen is chemically passive, colorless, odorless and tasteless. At 77.36 K and a pressure of 760 mm Hg, 1 liter of liquid nitrogen flashes to 650 l of gas. After usage the gaseous nitrogen is discarded in the environment, without any danger of suffocation for the workers.

The liquid can evaporate or not, but in either cases, the method has the main advantage of a great improvement of the heat transfer coefficient between the product to be frozen and the refrigerant.

Using cryogenic systems one can avoid the large investment required for a compression refrigeration system, using only from time to time cold delivery in the shape of the liquefied cryogenic fluid.

2. MATHEMEATICAL MODEL

Freezing is the process by which most of the water from the cellular liquid and the water from a product's tissues (capillary vases, intercellular spaces) is turned into ice. Water crystallization temperature ranges between -1…-5 °C, at which 60…75 % of the whole water content turns into solid.

The process must be continued afterwards by subcooling the product to a final temperature of -18…-25 °C, at which 90…95 % of the water content turns into solid. Thermal core temperature is a main indicator of the end of the freezing process as it can be with maximum 3…5 °C higher than the products' storage temperature.

International Institute of Refrigeration established the following conditions: final temperature of the products thermal core ≤ -15 ºC, average final temperature ≤ -18 ºC. Freezing process of a food product is a typically transient heat and mass transfer process. Transfer phenomenon is complex due to the phase change of the solidifying water and of the transport properties of the product (thermal conductivity, specific heat, etc.).

Computing methods use some simplifying assumptions which allow establishing some simple

calculus relations for the freezing duration (according to Plank):

- all the heat is drawn from the product at the freezing point temperature,
- the products are homogenous and isotropic,
- the cooling surroundings has a constant temperature,
- the product has already been cooled down to the freezing temperature.

Total duration of the freezing process is (Niculiță, P., Purice, N., 1986):

$$\tau_c = \tau_r + \tau_{cg} + \tau_{sr} \quad [s] \qquad (1)$$

where: τ_r [s] - primary refrigeration duration; τ_{cg} [s] - freezing duration; τ_{sr} [s] - product duration subcooling;

Primary refrigeration duration can be computed from the following relation:

$$\tau_r = \frac{m \cdot c}{\alpha \cdot s} \cdot \ln \frac{t_i - t_{mI}}{t_f - t_{mI}} \quad [s] \qquad (2)$$

$$m = \rho \cdot V \ [kg] \qquad (3)$$

$$V = \frac{4 \cdot \pi \cdot r_0^3}{3} \quad [m^3] \qquad (4)$$

where: m - product mass; ρ - density; c - specific heat; α - convection coefficient; s - product's external area; t_I - initial temperature; t_f - final temperature; t_{mI} - cooling surrounding temperature (zone I);

For a spherical shape product, freezing duration can be determined using Plank's formula (Porneală S., 2000):

$$\tau_{cg} = \frac{\rho \cdot l_{cg}}{t_{cg} - t_{mII}} \cdot \left(\frac{r_0^2}{6 \cdot \lambda} + \frac{r_0}{3 \cdot \alpha} \right) \qquad (5)$$

where: t_{cg} - freezing temperature; t_{mII} - cooling surrounding temperature (zone II); α - convection coefficient; r_0 - sphere radius; l_{cg} - freezing latent heat; ρ - density; λ - thermal conductivity;

The duration for subcooling of the frozen product to the final average temperature (t_{mf}) can be calculated using Plank's relation:

$$\tau_{sr} = 933 \cdot c_m \cdot n \cdot \left| \lg \frac{t_{cg} - t_{mIII}}{t_{III} - t_{mII}} - 0{,}0913 \right| \cdot \left(\frac{2 \cdot r_0}{\alpha} + \frac{r_0^2}{\lambda} \right) \cdot \frac{1}{3{,}6} \quad [h] \qquad (6)$$

where: c_m - frozen product average specific heat; n - dimensionless coefficient, whose values depends on the Biot dimensionless group, defined by:

$$Bi = \frac{\alpha \cdot \delta}{\lambda} \qquad (7)$$

where $\delta = r_0$.

Table 1.
Values for the dimensionless coefficient n vs. Bi [4]

Bi	0.25	0.5	1.0	2.0	4.0	10	∞
N	1.21	1.188	1.156	1.112	1.06	1.02	1.00

t_{cg} - freezing final temperature;

t_{mII} - cooling surrounding temperature (zone III);

t_{mIII} - thermal core final temperature of the product.

3. EXPERIMENTAL RESULTS

The paper analyses the freezing process duration for blueberries and raspberries. The products were frozen in a custom designed and built freezing tunnel. The cooling environment average temperatures (t_{mI}, t_{mII}, t_{mIII}) as well as the product temperatures (t_cg, t_{mIII}) were measured using digital display thermocouples.

Various properties of the considered products are presented in the following table.

Table 2.
Various properties of the considered products

Property\ Product	t_c [C]	c_{pI} [kJ/kgK]	c_{pIII} [kJ/kgK]	l_{cg} [kJ/kg]	λ [W/m-K]	ρ [kg/m^3]
Blueberries	-2.6	3770	1930	288.4	0.54	1000
Raspberries	-1.1	3520	1840	283.8	0.49	998

4. RESULTS AND DISCUSSION

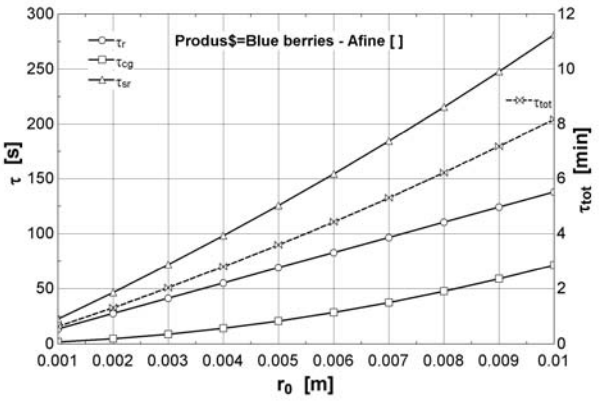

Fig.1 *Influence of product radius on partial and total freezing times*

As one can notice in Figure 1, increased size of products radius r_0 in the range of 1 … 10 mm

leads, as expected, to increased partial durations, and therefore an increased total duration for the entire freezing process. For the same product size, due to the different properties, blueberries have a slightly longer process time than raspberries (for the reference case with r_0 = 5e-03 m: $\tau_{tot\ blueberries}$ = 3.59 min, and $\tau_{tot\ raspberry}$ = 3.02 min) - see Figure 2.

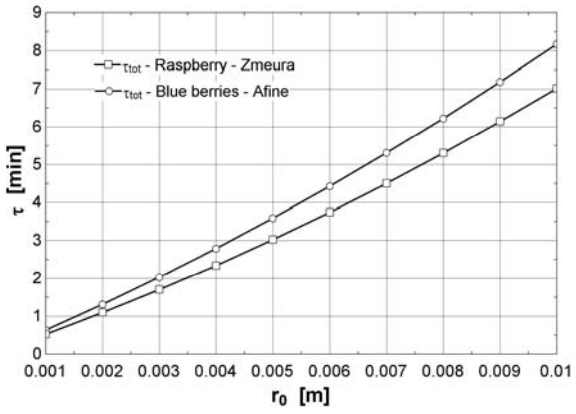

Fig. 2. *Total freezing time vs. product radius*

Fig. 3 shows the influence on convection coefficients $\alpha_{1,2,3}$ on corresponding process times. As it can be seen, the most powerful influence is the one of the cooling coefficient. Reference values were: α_1 = 35 W/m^2-K, α_2 = 530 W/m^2-K, α_3 = 25 W/m^2-K (Damian V., Vasilescu C., 1997).

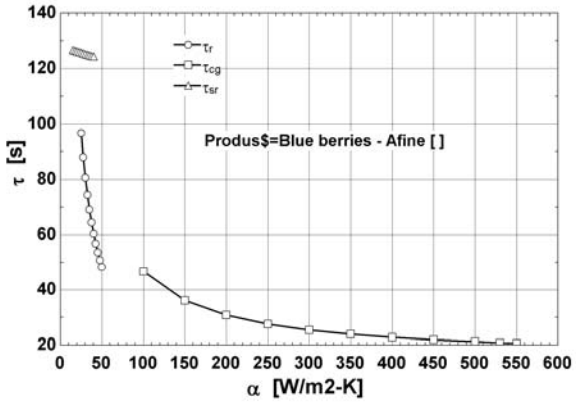

Fig. 3. *Influence of convection coefficients on corresponding times*

5. CONCLUSIONS

Considering some aspects concerning the environment and durable development (Carmen Cătălina Ioan, 2008), one may consider that this modern and environmentally friendly method of fast freezing using liquid nitrogen may be also used for other forest fruits (such as: underbrush, brambleberries, etc.) or various other food products.

The main **advantages** of liquid nitrogen freezing are:

- simple design, small space required and easy cleaning;
- short startup and freezing times, movable freezers can be designed;
- reduced weight losses;
- investment costs are with 50% smaller than for vapor compression systems, and there are no maintenance costs involved;
- the system can be used for various food products with no modifications;
- fully automation is possible, no defrost necessary (there are no evaporators);
- due to the high freezing speed, the formed ice crystals are very small and they do not damage the frozen products cells, thus keeping the initial color and taste; no preliminary product cooling is required;
- liquid nitrogen is obtained almost "for free" as an auxiliary product in oxygen production.

The main **disadvantage** of this freezing method is:

- energy consumption for production of gaseous nitrogen is 16.5 kWh/100 Nm^3 (Şerban A., Chiriac F., 2006) and the price of liquid nitrogen (at 77.36 K) is 0.3 €/l, therefore, the cost of cryogenic freezing using liquid nitrogen is just 7.3 % of total price of the frozen product (Damian V., Vasilescu C., 1997).
- the high cost of liquid nitrogen, but considering that freezing cost accounts only for 7,3 % of the product's price, one may disregard this disadvantage.

Acknowledgements: This work was supported by CNCSIS UEFISCSU, project number 501-PNII IDEI/2009.

REFERENCES

[1] Damian V., Vasilescu C., (1997), Criogenic freezing of meat products Congelarea criogenică a produselor din carne, (in Romanian), Ed. Evrika, Brăila, Romania

[2] Porneală S., (2000), Refrigeration and process air conditioning for food industry Tehnica frigului şi climatizării în Industria Alimentară, (in Romanian), Ed. Fundației Universitare "Dunărea de Jos", Galați, Romania.

[3] Niculiță P., Purice N., (1986), Refrigeration technologies in exploitation of animal origin food products Tehnologii frigorifice în valorificarea produselor alimentare de origine animală (in Romanian), Ceres Publishing House, Bucharest.
[4] Şerban A., Chiriac F., (2006), Technical Cryogenics, (in Romanian), AGIR Publishing House Bucharest.
[5] Ioan C. C., (2008), Awareness and development of the ecological attitude, key elements in education for sustainable development, The 8th International Conference of Technology and Quality for Sustained Development, AGIR Publishing House, Bucharest, ISSN: 1844-9158.
[6] Damian V., Iosifescu Cr., Coman G., (2005), Thermodynamics Termotehnica, (in Romanian), Ed. Academica, Galați, Romania.
[7] Brennan, James G., (2006), Food Processing Handbook, WILEY-VCH Verlag GmbH & Co. KGaA.
[8] Fellows, P., (2000), Food Processing Technology - Principles and Practice, 2nd Edition, Woodhead Publishing Limited and CRC Press LLC
[9] Hui, (2006), Handbook Of Fruits And Fruit Processing - Blackwell Publishing.

WATER VAPOURS HEAT PUMP FOR THE USE OF LOW ENTHALPY GEOTHERMAL RESOURCES

Sorin DIMITRIU

UNIVERSITY "POLITEHNICA" Bucharest, Romania

Rezumat. Lucrarea prezintă o posibilă soluție pentru creşterea eficienței sistemelor centralizate de alimentare cu energie termică. România posedă importante resurse geotermale. Acestea pot fi utilizate împreună cu sistemele clasice de încălzire utilizând cazane de apă fierbinte. Lucrarea propune o schemă de utilizare a resurselor geotermale de joasă entalpie, utilizând o pompă de căldură cu vapori de apă, pentru creşterea eficienței unui sistem centralizat de încălzire. Deşi vaporii de apă nu constituie un agent uzual, datorita inconvenientelor lor, în anumite condiții acest agent natural reprezintă o alternativă față de soluțiile clasice. Este prezentat un studiu de caz.
Cuvinte cheie: energie geotermală, pompă de căldură, eficiență energetică, apă geotermală.

Abstract. The paper presents a possible solution for the increasing of the efficiency of the centralized heating systems. Romania possesses important geothermal resources. These may be utilized in conjunction with the classical hot water boiler heating systems. The paper proposes a scheme to use the low enthalpy geothermal resources using a water vapours heat pump to increasing the efficiency of a centralized heating system. Although the water vapours are not an ordinary agent, due its inconvenient, in certain conditions this natural agent represent an alternative to conventional solutions. A case study is presented.
Keywords: geothermal energy, heat pump, energy efficiency, geothermal water.

1. INTRODUCTION

Romania has a high economic potential of the renewable energy sources. Among these, the geothermal energy resources - that were identified by drills – represent an annual potential of approximately $10 \cdot 10^6$ GJ (240000 tep - equivalent petroleum tons). By using approximately 60 functioning wells an annual contribution of $7 \cdot 10^6$ GJ (energy economy, equivalent to 167000 tep) is achieved [1], [2].

This energy is successfully used to produce thermal energy needed for technological processes, or, especially, for the heat supply of various residential areas. Only 2/3 of the existing potential is used in Romania, mainly because of the lack of a corresponding financial support, to sustain the development of this energy sector. In many cases, the exploitation of the geothermal potential is incomplete, the temperature of warm water to the outlet of the primary circuit of the heat exchangers being about 50°C. This water, normally discharged to the waste channel or injected in the geothermal deposit, can be utilized as a low enthalpy source from a heat pump.

The present paper proposes such modern and unconventional solution for the utilisation of the energy potential of the low enthalpy geothermal water or other resources in order to prepare thermal agent from a centralized heating system.

2. THE OPERATING PRINCIPLE OF THE WATER VAPOURS HEAT PUMP.

Figure 1 shows schematic diagram of the one stage water vapours heat pump (WVHP). The water with low temperature t'_{gw} from the geothermal deposit, or residual water from the heat exchangers, used as heat source comes in the evaporator recipient trough an expansion valve. The water pressure is reduced by throttling to the saturation pressure corresponding to the desired temperature t''_{gw}, a partial vaporisation process appearing. The gaseous phase is taken by the turbo-compressor and the liquid phase is pumped out. The compressed vapours, with high temperature, are introduced in the condenser, with the water to be heated. The operating pressure of the condenser is the saturation pressure corresponding to temperature t'_{hw} of the hot water

pumped to the heat consumer. It highlights the following features of the scheme: the open circuit of the working agent and the mixing heat exchange in evaporator and condenser [3], [4], [5].

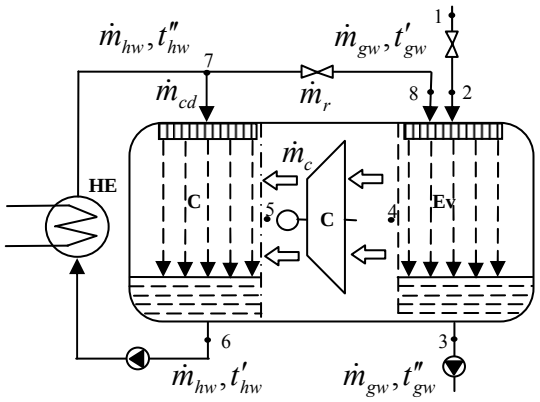

Fig.1. *The schematic diagram of the one stage WVHP.*
C- compressor; Cd-condenser; Ev-evaporator; HE-heat exchanger

The drawbacks of using water as refrigerant are: very high specific volume at compressor suction, high compression ratio and high temperature at the compressor outlet and high compression mechanical work. There are also problems of corrosion which make necessary the use of titanium or composite materials for compressor impeller. Working under vacuum, the forces exerted by the gas on the blades are very small, operating speed of rotation can reach 10 000 rpm and tip peripheral velocity 500 m/s [7], [8]. In such conditions the maximum compression ratio can not exceed 4…5, which corresponds to a temperature difference of about 25…30 ^{o}C between condenser and evaporator. For larger temperature differences, i.e. higher compression ratios, it is necessary to use a multi-stage compressor.

Figure 2 shows the schematic diagram of a two stages WVHP. Between the two stages of the compressor is introduced a mixing heat exchanger. The vapours delivered from the first stage of the compressor are cooled to saturation state using the liquid taken from the return line of the heat consumer. The resulting saturated liquid is driven to evaporator. In this way the compression work is reduced and the efficiency increases. The heat consumer circuit is fed with the saturated liquid taken from the condenser.

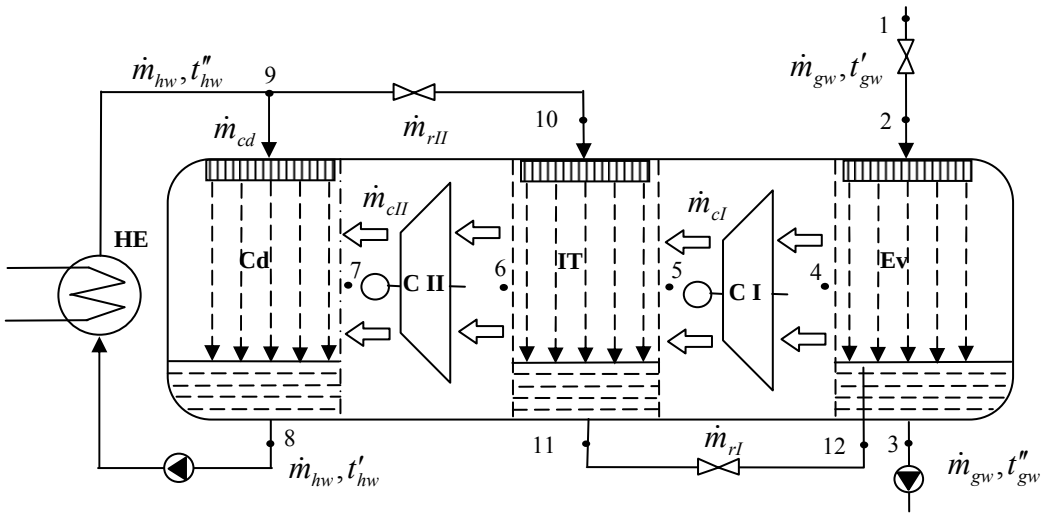

Fig.2. *The schematic diagram of the two stages WVHP.*
Cd - condenser; Ev - evaporator; IT - intermediate tank; CI - first stage compressor; CII - second stage compressor; HE - heat exchanger.

3. MATHEMATICAL MODEL OF ONE STAGE WVHP [5], [6]

The operating pressure of the evaporator is determined by the temperature t''_{gw} of the geothermal water pumped out from recipient:

$$p_v = p_s(t''_{gw}) \text{ [bar]} \qquad (1)$$

From the mass and energy balance equations of the evaporator, the compressor mass flow results:

$$\dot{m}_c = \dot{m}_{gw} \frac{h_2 - h_3}{h_4 - h_8} \text{ [kg/s]} \qquad (2)$$

The operating pressure of the condenser is determined by the temperature t'_{hw} of the heat water that feeds the consumer:

$$p_c = p_s(t'_{hw}) \text{ [bar]} \qquad (3)$$

From the mass and energy balance equations of the condenser, the hot water mass flow results:

$$\dot{m}_{hw} = \dot{m}_c \frac{h_5 - h_7}{h_6 - h_7} \quad [\text{kg/s}] \tag{4}$$

respectively the recycled mass flow:

$$\dot{m}_r = \dot{m}_c \tag{5}$$

The electric power of compressor is:

$$P = \dot{m}_c (h_5 - h_4) \quad [\text{kW}] \tag{6}$$

and the heat exchanges made with the cold source, respectively the hot are:

$$\dot{Q}_{SR} = \dot{m}_{gw} (h_2 - h_3) \quad [\text{kW}] \tag{7}$$

$$\dot{Q}_{SC} = \dot{m}_{hw} (h_6 - h_7) \quad [\text{kW}] \tag{8}$$

The compression process is considered adiabatic, no isentropic. The real state at the compressor discharge is determined by the isentropic efficiency, expressed according to the polytropic efficiency value, set to 0.8:

$$\eta_{is} = \frac{\varepsilon^{\frac{k-1}{k}} - 1}{\varepsilon^{\frac{n-1}{n}} - 1} \tag{9}$$

$$\frac{n-1}{n} = \eta_{pol} \frac{k-1}{k} \tag{10}$$

where ε is the compression ratio.

The isentropic exponent k is determined based on the isentropic compression process, considering water vapours in ideal gas state:

$$\frac{k-1}{k} = \frac{R(T_{5s} - T_4)}{h_{5s} - h_4} \tag{11}$$

The COP of the one stage WVHP will be:

$$COP = \frac{\dot{Q}_{SC}}{P} \tag{12}$$

4. MATHEMATICAL MODEL OF TWO STAGES WVHP.

The conditions that lead to condensation and evaporation pressures are the same as for the one stage WVHP. The intermediate pressure is expressed classically:

$$p_i = \sqrt{p_v \cdot p_c} \quad [\text{bar}] \tag{13}$$

From the mass and energy balance equations of the evaporator, the first stage compressor mass flow results:

$$\dot{m}_{cI} = \dot{m}_{gw} \frac{h_2 - h_3}{h_4 - h_{12}} \quad [\text{kg/s}] \tag{14}$$

The recycled mass flow from the intermediate tank is:

$$\dot{m}_{rI} = \dot{m}_{cI} \quad [\text{kg/s}] \tag{15}$$

From the mass and energy balance equations of the intermediate tank, the second stage compressor mass flow results:

$$\dot{m}_{cII} = \dot{m}_{cI} \frac{h_5 - h_{11}}{h_6 - h_{10}} \quad [\text{kg/s}] \tag{16}$$

The recycled mass flow from condenser is:

$$\dot{m}_{rII} = \dot{m}_{cII} \quad [\text{kg/s}] \tag{17}$$

From the mass and energy balance of the condenser, the mass flow for cooling is:

$$\dot{m}_{cd} = m_{cII} \frac{h_7 - h_8}{h_8 - h_9} \quad [\text{kg/s}] \tag{18}$$

The hot water mass flow will be:

$$\dot{m}_{hw} = \dot{m}_{cII} \frac{h_7 - h_9}{h_8 - h_9} \quad [\text{kg/s}] \tag{19}$$

The compression processes are also considered adiabatic, no isentropic. The real states at the compressor discharges are determined by the isentropic efficiency, the same as for the one stage WVHP.

The electric power of the compressors is:

$$P_I = \dot{m}_{cI} (h_5 - h_4) \quad [\text{kW}] \tag{20}$$

$$P_{II} = \dot{m}_{cII} (h_7 - h_6) \quad [\text{kW}] \tag{21}$$

$$P = P_I + P_{II} \quad [\text{kW}] \tag{22}$$

and the heat exchanges made with the cold source, respectively the hot will be expressed:

$$\dot{Q}_{SR} = \dot{m}_{gw} (h_2 - h_3) \quad [\text{kW}] \tag{23}$$

$$\dot{Q}_{SC} = \dot{m}_{hw} (h_8 - h_9) \quad [\text{kW}] \tag{24}$$

The COP of the two stage WVHP will be:

$$COP = \frac{\dot{Q}_{SC}}{P} \tag{25}$$

5. RESULTS AND DISCUTIONS.

Based on the mathematical models presented above, a simulation of the two stages WVHP operation was carried out, in different conditions utilising the EES software. The simulation was performed for a water volume flow of the cold source of 1 m^3/min. The temperature difference between inlet and outlet water of 10 degrees was considered for both condenser and evaporator as well. The polytropic efficiency was set to 0.8 for all regimes. The isentropic exponent was established along the isentropic compression process for each stage of the compressor.

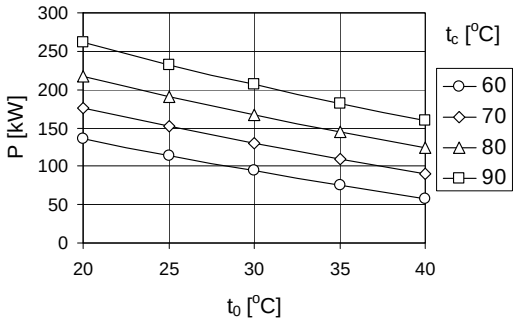

Fig.3. *The power consumed by the compressors.*

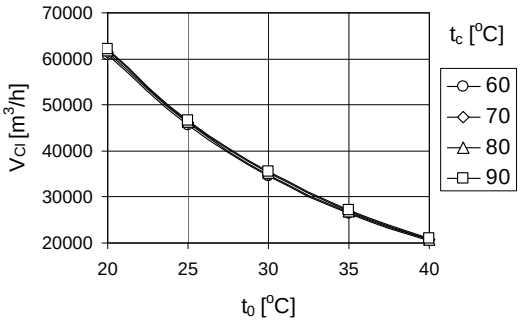

Fig.6. *The flow volume aspirated by the first stage of the compressor.*

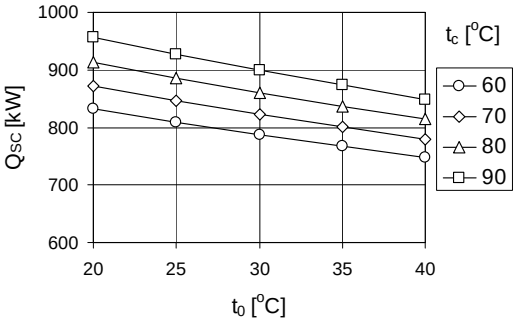

Fig.4. *The heat flux transferred to the hot source*

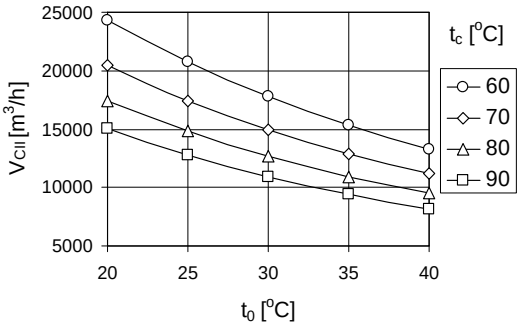

Fig.7. *The flow volume aspirated by the second stage of the compressor.*

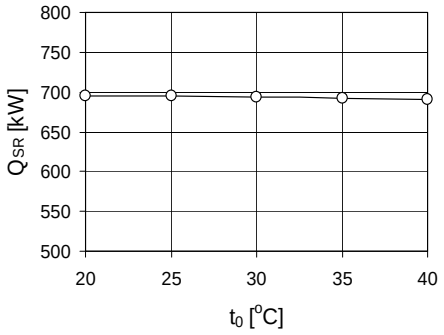

Fig.5. T*he heat flux over the cold source*

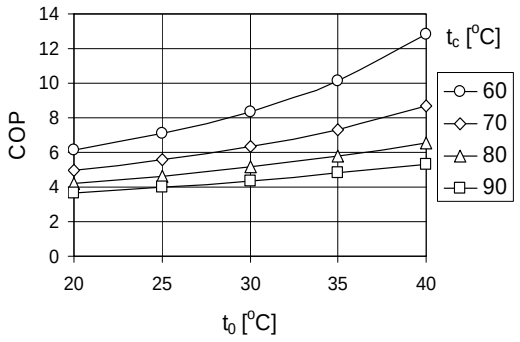

Fig.8. *The COP of installation.*

The figures 3...8 show the operation characteristics of the installation depending on the evaporation and condensation temperature and its efficiency. The evaporator thermal load is constant because of the constant water flow over the source.

The flow volume aspirated by the compressor first stage does not depend on the condensation temperature, but only the evaporator operating conditions. Increasing of the condensation temperature increases the suction pressure of the compressor second stage, and decreases the suction volume flow. The plant efficiency depend both the evaporation and condensation temperature, and the temperature difference between the inlet and outlet water from these recipients. It highlights the high values of the plant efficiency, about 5…8, for the vaporization temperatures in range of 30…40 ^{o}C and the condensation temperatures in range of 70…80 ^{o}C. This area corresponds to conditions of the use for heating.

These results highlight the fact that WVHP has an equal and even higher efficiency compared to plants using classical agents. Furthermore, the water is a natural refrigerant, absolutely harmless to man and nature. It is easily available, and there are not problems disposing it after use. Even

though water is one of the oldest refrigerants, it requires state-of-the-art technology to use as refrigerant in heat pumps or chillers due some specific features. Since the cycle works under high vacuum, volumetric cooling capacity of water vapours is very low and huge volume flows have to be compressed with relative high pressure ratios. Compared with classical agents such as R134a or R12, the use of water as refrigerant causes approximately a 200 times higher volume flow and a double pressure ratio for the same application [9]. This high pressure ratio requires a peripheral speed approximately 2 to 4 times higher, depending on the impeller design. High pressure ratio can be obtained using a combination of high rpm and large diameter, where the diameter is primarily limited by the available space and manufacturing facility. New technologies have been developed recently, for the design and manufacture of the impellers from titanium, composite materials or carbon fibres. Figure 9 shows such a rotor which is 1 m in diameter and has operating speed of 10 000 rpm.

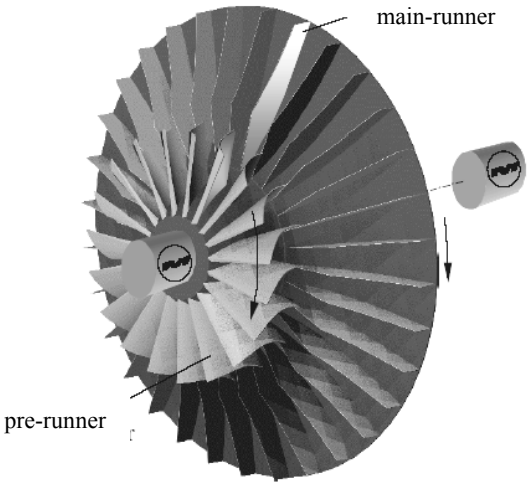

Fig.9. *Combined impeller for water vapours centrifugal turbo-compressor* [7]

This impeller is composed from two parts on the same shaft: an inducer with curved blades (pre-runner) and an open rotor with radial blades (main-runner). Both impellers rotate in the same direction, and there are not guide vanes between them. The inducer usually has a smaller diameter, and in order to obtain an even higher work transmission, can be cut off the main shaft and driven separately at the highest rpm allowable by stability or Mach number limit considerations. The flow volume can be about 200 000 m^3/h [7].

A prototype turbo compressor system has been installed at the LEGO factory in Denmark. This uses a two-stage centrifugal turbo-compressor to compress the very high volume of water vapour needed for its 2 MW cooling capacity. As a prototype the cost of the system was very high, at around 7500 USD/kW compared to 80-160 USD/kW for the conventional chillers. However, its COP is claimed to be higher than the conventional R22 chillers. This prototype has 8.5 m long, 3.6 m height and 10 tons weight. Similar chillers were installed at University of Essex (U.K) and Institut für Luft- und Kältetechnik Dresden (Germany) [10].

Figure 10 shows the chiller installed at the University of Essex.

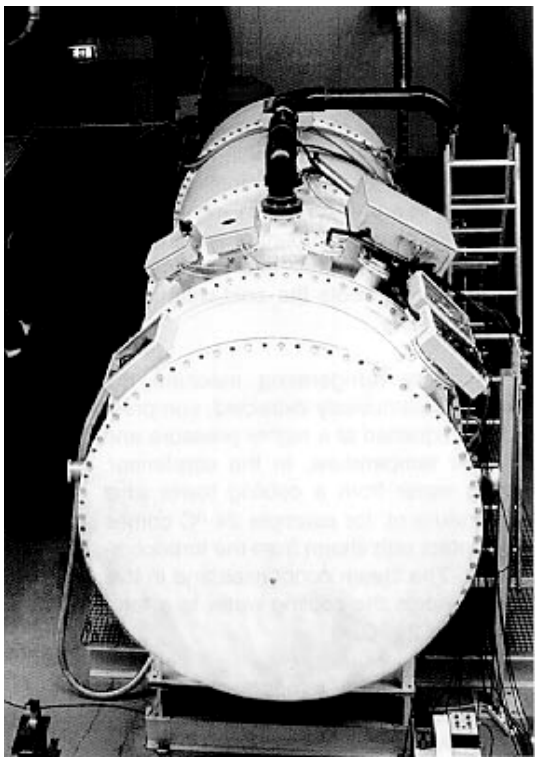

Fig.10. *Water vapours chiller with two stages centrifugal compressor (University of Essex -U.K.)*

A consortium of some Japanese companies has completed recently a prototype of water vapours chiller incorporating an axial turbo-compressor, with 1,6 MW cooling capacity. This prototype, that utilizes direct heat exchangers, has achieved significant downsizing and has a footprint approximately on-third that of a conventional water vapours chiller utilizing a centrifugal compressor [11].

This results and achievements demonstrate that the water vapours can be utilised as refrigerant in applications such as heat pumps and chillers, in conditions of high efficiency, equal and even higher than similar classical installations. Even if

the price of investment is nowadays still prohibitive, the development of the technologies, and the need to respond to environmental conditions becoming more severe, make these systems a solution for the future [9].

6. CAS STUDY

A case study was conducted on the use WVHP to increase energy efficiency of centralized heat supply system of the city Calimanesti, Valcea County [12]. The thermal energy necessary for the system is obtained from the geothermal water from a well drilled on the right bank of the Olt River.

Geothermal water is cooled in a heat exchanger to prepare hot water for the heating system, and then is discharged directly into the Olt River. Because the operating conditions, the geothermal water can not cool below the temperature of 50°C, its energy potential being used incomplete. To turn to the best account the thermal potential of the geothermal water, it was proposed a solution to recover the available thermal energy from the water discharged in the Olt River, by using a heat pump [13]. The figure 11 shows the insertion of the heat pump in the functioning scheme of the geothermal station of the town Calimanesti.

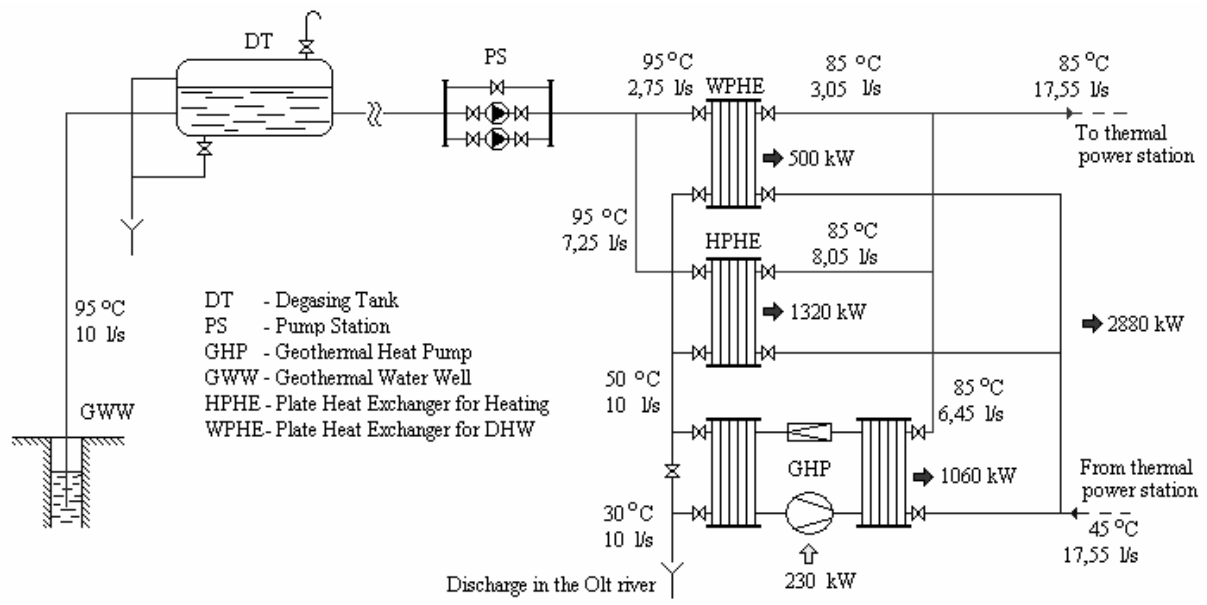

Fig.11. *The scheme of geothermal station with GHP heat recovery*

In the heat pump evaporator, the geothermal water is cooled off to a temperature of about 30°C, after that being discharged in the Olt River. The heat pump condenser operates in parallel with the geothermal water heat exchanger, multiplying the thermal fluid flow sent into the thermal energy supply system, therefore increasing the heat provided to the system. In this way, it can be covered about 2/3 from the estimated thermal energy needs. The rest of thermal energy and the peaks are covered by hot water boilers using liquid fuel. Operation of the plant was studied considering as refrigerant R123 and water vapours (R718) as an alternative.

When was used as refrigerant R123, was considered a one-stage mechanical vapour compression heat pump. If water vapours, is necessary to use a two-stage compression system. In this case, the heat exchangers operate in vacuum conditions, and for this reason the evaporator can be a direct heat exchanger, but the condenser must be an indirect heat exchanger or must be attached to a surface heat exchanger. Figure 12 presents the results obtained using EES software for R718 (water vapours), while Table 1 shows the comparative results for the two agents in the same conditions.

Comparing the results for the two agents can be seen that performance is similar. When using water vapours, the plant efficiency significantly depends on the value of the polytropic efficiency. For example, increasing the compressor polytropic efficiency from 0.8 to 0.9, the COP increases from 4.632 to 4.913, which is higher than when using R123 as refrigerant. As a result, the compressor appears to be the key of the superior performances.

The current researches promise the development of high performance compressors, carbon fibres rotors, which will lead to the development of highly efficient equipments.

Although at present is still a very high investment cost of WVHP, the equipments being in the prototype phase, there is the hope to reduce in the future their cost to the level of the traditional installations

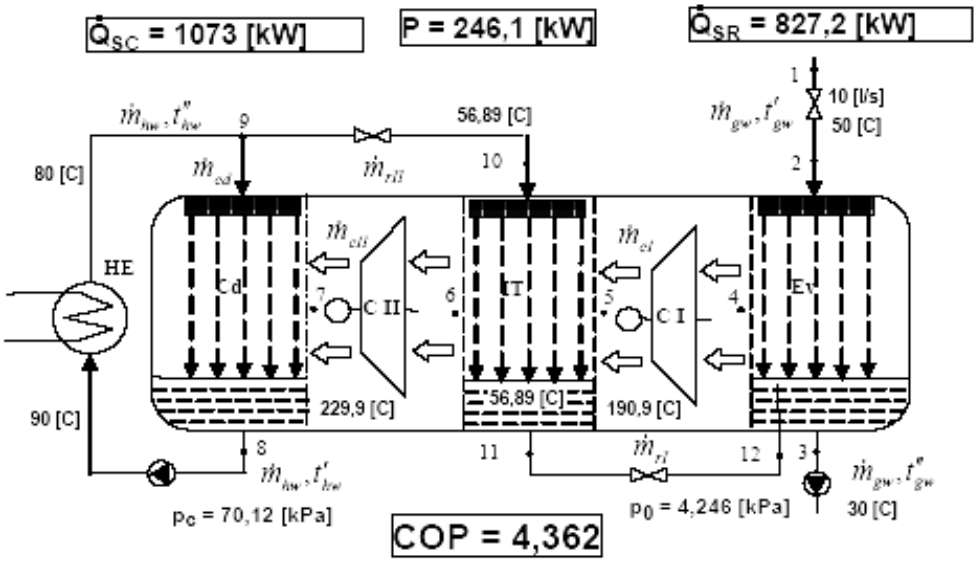

Fig.12. *The result of simulation using EES software.*

Table 1

Characteristic parameters of the installation

Parameter	Value	
	R718	**R123**
Vaporisation pressure [kPa]	4.25	91.5
Condensation pressure [kPa]	70.12	625.2
Compression ratio	16.5	6.8
Vaporisation temperature [^{o}C]	30	25
Condensation temperature [^{o}C]	90	90
Evaporator load [kW]	827	1073
Condenser load [kW]	827	1060
Compression power [kW]	246	230
Efficiency (COP)	4.362	4.608
First-stage volume flow [m^3/min]	705	59.25
Second -stage volume flow [m^3/min]	218	-

The case study presented demonstrates that the water vapours heat pump can be successfully utilised for the recovery of the heat sources with low thermal potential. In addition, these plants are totally "green" using as refrigerant a natural and completely innocuous agent.

7. REFERENCES

[1] ISPE - S*trategia de valorificare a surselor regenerabile de energie din România*, Studiu nr. I-475.13.001-B0-002, 2007.

[2] ICEMENERG - *Studiu privind evaluarea potențialului energetic actual al surselor regenerabile de energie în România - solar, vânt, biomasă, microhidro, geotermie-, identificarea celor mai bune locații pentru dezvoltarea investițiilor în producerea de energie electrică neconvențională*, Raport cercetare, 2006.

[3] Radcenco, Vs., Dimitriu, S., ş.a.: *Cercetări privind schemele şi echipamentele necesare instalațiilor de pompe termice necesare pentru valorificarea resurselor geotermale din România.* In: Raport de cerc. UPB nr. 115, 1973.

[4] Radcenco, Vs., Florescu, Al., Dimitriu, S., s.a. - *Instalatii de pompe de caldura*, Editura Tehnică, Bucureşti, 1985.

[5] Dimitriu, S.- *Posibilități de valorificare a resurselor geotermale cu ajutorul unei pompe de căldură cu vapori de apă*. In: CD a XV-a Conf. Int. de Termotehnică, 26-28 mai, Craiova, 2005.

[6] Dimitriu, S. - *Pompa de căldură cu apă – o posibilă soluție pentru valorificarea resurselor geotermale.* In: CD a XV-a Conf. CECEPM, 26-27 nov, UTCB, Fac. Instalații, Bucureşti , 2008.

[7] Müller, N. - *Design of Compressor Impellers for Water as a Refrigerant.* In: ASHRE Transaction, Vol 107, pp. 214-222.

[8] Müller, N. - *Turbo Chillers using Water as Refrigerant*. In: ASME Process Industry Division PID Newsletter, Fall 2002, pp. 3.

[9] Kilicarlsen, A., Müller, N. - *COPs of R718 în Comparation with Other Modern Refrigerants.* In: Proceed. of the 1-th Cappadocia Int. Mech. Eng. Symp., 14-16 July, Cappadocia , pp. 317-323 , 2004.

[10] Kühn-Kinel J. - *New age water chillers with water as refrigerant* - CERN, Geneva, 1997

[11] Tokyo Electric Power Company - TEPCO - *Development of World's First Water Vapor Chiller with Axial Compressor*, Press Release,19 Jan, 2011.

[12] Burchiu, N., Burchiu, V., Gheorghiu, L. - *Centralized heat supply system based on geothermal resources, in Calimanesti, Valcea County*, Proceedings of the 4th National Conference of the Hydroenergeticians from Romania, 2006.

[13] Bianchi A.M., Dimitriu S., Stanciu D., Băltăreţu F., - *Geothermal Energy Utilization for Increasing of the Energy Efficiency of a District Heating System* - Clima 2010-10th REHVA World Congress 9-12 Mai 2010, Antalya-Turkey, Abstr. Book pp.178-17

NUMERICAL MODELING OF BINARY ICE GENERATOR

Mădălina Teodora Nichita[1], Anica Ilie[1], Florea Chiriac[1], Viorel Popa[2]

[1]TECHNICAL UNIVERSITY OF CIVIL ENGINEERING, BD.PACHE PROTOPOPESCU NO 66,, 021414, BUCHAREST
[2]UNIVERSITY "DUNAREA DE JOS", 111 STR. DOMNEASCA, GALATI,

REZUMAT: În această lucrare se prezintă modelarea teoretică a unui generator de gheață. În raport cu agenții frigorifici clasici, gheața binară reprezintă un agent intermediar, cu schimbare de fază care îl recomandă pentru diferite aplicatii.

În lucrare se evidențiază modelarea teoretica a două generatoare de gheață binară de 1 kW ce utilizează amoniacul și a altui generator de 7kW ce utilizează freonul R404A.

În plus autorii analizează comparativ aceste două generatoare cu o a treia varianta, rezultată experimental, în care generatorul are o putere frigorifica de 8.9kW, puterea de comprimare fiind măsurată.
Cuvinte cheie: generator de gheață binară, agent frigorific, gheață binară, aer condiționat

ABSTRACT: This paper presents a theoretical modeling of ice generator refrigerants in relation to classical ice slurry is an intermediate agent, phase change that is recommended for different applications.

The paper highlights the theoretical modeling of second-generation 1 kW ice slurry that use ammonia and other generator that uses freon R404A 7kW.

In addition the authors analyze these two generators compared with a third alternative, experimental results, the generator has a cooling power of 8.9kW, power compression is measured.
Keywords: ice-slurry generator, refrigerant, ice-slurry, comfort air-conditioning

1. INTRODUCERE

Ice slurry (ice-slurry - in english, coulis de glace - french) is a suspension of fine particles of ice (0.01 ÷ 0.2) mm in an aqueous solution (water plus additives to lower the freezing point of water: alcohol, glycol, salt). Ice slurry thermodynamic properties and has good high enthalpy water mass, being used both as an intermediary agent and as a cold storage medium. Ice slurry has established itself as an intermediary agent and media in the last 15 years. It is a natural agent, organic, inexpensive and high latent heat content (binary mixture liquid-solid two-phase state). If air conditioning use ice slurry to obtain significant energy savings compared to chilled water systems and water cooled with ice.

In terms of geometric configurations, ice slurry generator consists of two concentric tubes and a device for scraping the ice consists of a central shaft (driven by an electric motor) on which is fixed length tape scraping helical form.

2. CALCULATION ALGORITHM FOR ICE SLURRY GENERATOR

For ice slurry generator sizing is necessary, first step, the determination of heat transfer coefficients, both working on the agent (ethylene glycol aqueous 1% by weight), which solidifies and makes ice on the inner surface of the cylinder inside, as and the refrigerant (R404A freon and ammonia), which evaporates in the intratubular space.

To determine the convective heat transfer coefficient, on the binary ice was used empirical relation for Nusselt number specifies generation of binary ice by scraping (with a screw scraper), indicated by Bel et al. (1996):

$$Nu_i = \frac{\alpha_i \cdot (d_i - d_r)}{\lambda_{gb}} = (\mathrm{Re}_{rad} + \mathrm{Re}_{axial})^{0.245} \cdot \mathrm{Pr}^{0.142} \quad (1)$$

where: α_i = coefficient of convective heat transfer inside, [W/m^{2}K]; d_i = inner diameter pipe, [m]; d_r = outside diameter of the rotor, [m]; λ_{gb} = oefficient of thermal conductivity of ice slurry, [W/mK]; Re_{rad} = radial Reynolds number, corresponding to rotational speed, [-]; Re_{axial} = axial Reynolds number, corresponding to axial velocity, [-]; Pr = Prandtl number, [-].

Thermophysical properties contained in (1) were calculated from the average temperature of biphasic mixture. To calculate the coefficient of thermal conductivity of ice slurry, λ_{gb}, was used relatively Berg (1995, 1999), based on Jeffrey's model (1973) which takes into account the thermal interaction between particles of ice:

$$\lambda_{gb} = \lambda_l \cdot \left[1 + 3 \cdot \varphi \cdot \beta \cdot \left(1 + \varphi \cdot \beta \cdot \gamma\right)\right] \qquad (2)$$

where: λ_l = thermal conductivity of ethylene glycol aqueous solution 1%, [W/mK];

$$\varphi = f \cdot \frac{\rho_l}{\rho_g} \qquad (3)$$

where: ρ_l = density of 1% ethylene glycol aqueous solution, [kg/m^3]; ρ_g = ice density, [kg/m^3].

$$\beta = \frac{\chi - 1}{\chi + 2} \qquad (4)$$

where: $\chi = \frac{\lambda_g}{\lambda_l}$; λ_g = thermal conductivity of ice, [W/mK];

$$\gamma = 1 + 0{,}25 \cdot \beta + \frac{3 \cdot \beta}{16} \cdot \left(\frac{\chi + 2}{2 \cdot \chi + 3}\right) \qquad (5)$$

Fraction of ice, f, the solution may be around 25-30% (optimal value), depending on operational conditions of the ice generator (eg. the solution flow rate, solution concentration, time of formation of ice crystals transfer of heat between the refrigerant and binary solution). Accordingly they adopted the value of 30%. Ice density can be evaluated by Bell (1999) (which established a relationship with water-ethanol binary mixture based on the experimental data of Perry (1973) and Oliveras (1989) and taking into account the extrapolation of data from the literature up to temperature eutectic after Levi's relationship:

$$\rho_g = 917 \cdot \left(1 + 1{,}73 \cdot 10^{-4} \cdot \theta\right), \text{[kg/m}^3\text{]} \qquad (6)$$

where: θ = ice slurry temperature, [°C];

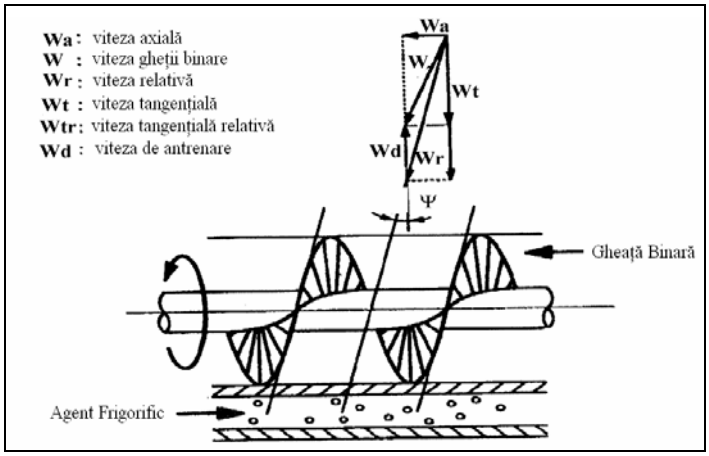

Figura 1. Scraped surface ice-slurry generator scheme

Re_{rad} = radial Reynolds number, corresponding to the speed of rotation of the tangential component of the spiral by, w_t, was calculated as (Bel and others 1996) with relation (figure 1):

$$\mathrm{Re}_{rad} = \frac{\rho_{gb} \cdot w_t \cdot d_i}{\eta_{gb}}, \text{[-]} \qquad (7)$$

where: ρ_{gb} = ice slurry density [kg/m3], calculated with the relationship:

$$\rho_{gb} = \left[\frac{f}{\rho_g} + \frac{1 - f}{\rho_l}\right]^{-1} \qquad (8)$$

$$w_t = +w_d + w_a \cdot \cot an\Psi \qquad (9)$$

where: w_d = crew the drive speed [m/s] was calculated with relation:

$$w_d = \frac{\pi \cdot d_i \cdot n}{60}; \qquad (10)$$

where: n = screw speed, [rot/min]; w_a = axial velocity of the binary ice [m/s] was calculated with relation:

$$w_a = \frac{4 \cdot \dot{D}_{vgb}}{\pi \cdot \left(d_i^2 - d_r^2\right)}; \qquad (11)$$

where: $\dot{D}_{vgb}$ - volume flow of ice slurry, [m^3/h]; d_r = - diameter rotor, [m]; Ψ = angle of the blade, 10°; η_{gb} = dynamic viscosity of ice slurry, [Pa s], calculated by Bell, Ben Lekhdon was based on liquid phase viscosity, as amended by a factor depending on the volume fraction of solid, the relationship:

$$\eta_{gb} = \eta_l \cdot \left(1 + 2.5 \cdot \varphi + 10.05 \cdot \varphi^2 + 0.00273 \cdot e^{16.6 \cdot \varphi}\right) \quad (12)$$

where: η_l = dynamic viscosity of 1% ethylene glycol aqueous solution, [Pa s]; $\eta_l = 0.0025$ [Pa s];

Re_{axial} = axial Reynolds number, the corresponding axial velocity was calculated as (Bell and others, 1996) with relationship:

$$\mathrm{Re}_{axial} = \frac{\rho_{gb} \cdot w_a \cdot \left(d_i - d_r\right)}{\eta_{gb}} \quad (13)$$

Pr = Prandtl number, calculated by the relationship:

$$\mathrm{Pr} = \frac{\eta_{gb} \cdot c_{pgb}}{\lambda_{gb}}, \quad (14)$$

where: c_{pgb} - specific heat of ice slurry, [J/kg k], relationship was determined:

$$c_{pgb} = c_{pg} \cdot f + c_{pl} \cdot (1 - f) \quad (15)$$

where: specific heat of 1% ethylene glycol aqueous solution; c_{pg} = specific heat of ice, $c_{pg} = 2101 J/kgK$. Specific heat of ethylene glycol aqueous solution 1% in average temperature of - 2 °C is 4212 J/kg K (by Ashrae Fundamentals 2010).

2.1. Assumptions for calculation

- cooling power plant (with ammonia) to generate ice slurry, $\Phi_o = 1000W$;
- cooling power plant (with freon) to generate ice slurry, $\Phi_o = 7000W$;
- screw speed: $n = 100\, rot/\min$;
- spiral angle of the blade: $\Psi = 10^o$;
- ice slurry mass fraction ice, $f = 0.30$ latent heat yields across the consumer, so that the consumer return pipe ice fraction is null;
- ice slurry mass flow is calculated with the relationship: $Q_{gb} = \frac{1}{f} \cdot \frac{\Phi_0}{r_s}$, [kg/s];

where: r_s = latent heat of solidification of ethylene glycol aqueous solution 1%, [J/kg]; r_s = 333000J/kg.

Ice slurry flows resulting $Q_{gb} = 0{,}01\ kg/s$ for generating plant with ammonia and ice slurry flow: $Q_{gb} = 1.60\, m^3/h$ for generating plant with Freon.

2.2. Calculation of thermophysical and transport measurements

2.2.1. Convective heat transfer coefficient, α_0, the vaporization of ammonia (to use his relationship Krujilin):

$$\alpha_0 = 4.2 \cdot \left(1 + 0.007 \cdot \theta_0\right) \cdot q_0^{0.7}, \text{ [W/m}^2\text{ K]}, \quad (16)$$

where: θ_0 - vaporization temperature, [°C]; q_0 - uniform heat flux of vaporization, [W/m^2].

Since the heat flow to the vaporization of ammonia unit in tight spaces is, typically, values in the range (1500÷3000)W/m^2, be adopted – in a first step, the value of 1550 W/m^2, it will be recalculated to achieve a relative error less than 4%.

For a vapor temperature $\theta_0 = -10^0 C$, application of relationship (16) lead to: $\alpha_0 = 668{,}27 \left[W/m^2 K\right]$

2.2.2. Convective heat transfer coefficient, α_e, the vaporization of Freon (to use his relationship Chawla):

$$\alpha_e = A_V \cdot \frac{m^{0.1} \cdot q_p^{0.7}}{d_i^{0.7}}, \text{ [W/(m}^2\text{*K)]} \quad (17)$$

$$A_v \cong \pi_o^{1/8} \cdot \frac{0.79}{\mu^{0.35}}, \text{ [W}^{0,5}\text{*m}^{0,14}\text{*s}^{0,2}\text{/(kg}^{0,1}\text{*grd)]}$$

where: μ = molecular mass of refrigerant for freon R404A, $\mu = 97.6\ kg/kmol$; $\pi_o = \frac{p_o}{p_{cr}} =$ the relationship between vapor pressure and critical pressure; $p_{cr} = 37.35 bar$; θ_0 = freon is the vaporization temperature, θ_0 = -5 °C, so $p_o = 4.96 bar$; q_0 = uniform heat flow, q_0 = 2000 W/m^2, guide is chosen in 1500 ÷ 3000 W/m^{2}but it will be recalculated to meet the condition of relative error <4% (with more tests, and it was last exact value). This results: $\alpha_e = 821.12 W/m^2 K$.

2.2.3. Overall heat transfer coefficient, k,

between this agent and ammonia / freon was determined by the relationship:

$$k = \frac{1}{\frac{1}{\alpha_i} + \frac{\delta_g}{\lambda_g} + \frac{d_e - d_i}{\lambda_{otel/cupru}} + \frac{1}{\alpha_0}} \quad (18)$$

where: α_i = heat transfer coefficient on the ice slurry, [W/m^2 K]; δ_g = thickness of ice deposited on the inner wall of the cylinder, [m]; λ_g = thermal conductivity of ice, [W/mK]; d_e, d_i = outer diameter steel pipe inside that, [m];

$\lambda_{otel/cupru}$ = thermal conductivity of steel. [W/mK].

2.2.4. The calculation of logarithmic mean temperature

Logarithmic mean temperature, Δθm [° C] is calculated with the formula:

$$\Delta\theta_m = \frac{\left(\theta^1_{gb} - \theta_0\right) - \left(\theta^2_{gb} - \theta_0\right)}{\ln \frac{\left(\theta^1_{gb} - \theta_0\right)}{\left(\theta^2_{gb} - \theta_0\right)}}, \text{[K]} \qquad (19)$$

where: $\theta^1_{gb}, \theta^2_{gb}$ = ice slurry temperature at the joining, or leaving the generator, [°C]; θ_0 = evaporation temperature of ammonia / freon, [°C].

2.2.5. Calculation of heat transfer surface

Heat transfer surface between the agent evaporates and ice slurry is determined by the relationship:

$$S = \frac{\Phi_0}{k \cdot \Delta\theta_m}, \text{[W]} \qquad (20)$$

Applying the calculation relationships above resulted ventilation and geometrical sizes summarized in table 1. Meanwhile, in table 1 are presented the experimental results obtained from the binary ice generator with freon.

Table 1. Heat transfer characteristics and geometry of the binary ice generator

Binary ice generator with ammonia	**Freon binary ice generator**	**Freon binary ice generator (experimental)**
Cooling power: $\Phi_0 = 1kW$	Cooling power: $\Phi_0 = 7\,kW$	Cooling power: $\Phi_0 = 8.90\,kW$
Vaporization temperature of the refrigerant: $\theta_0 = -10^0 C$	Vaporization temperature of the refrigerant: $\theta_0 = -6^0 C$	Vaporization temperature of the refrigerant: $\theta_0 = -18^0 C$
Ice slurry temperature: $\theta_{gb} = -2^0 C$	Ice slurry temperature: $\theta_{gb} = -2^0 C$	Ice slurry temperature: $\theta_{gb} = -2.2^0 C$
Logarithmic mean temperature difference between working units of generator: $(\Delta\theta)_m = 7.95^0 C$	Logarithmic mean temperature difference between working units of generator: $(\Delta\theta)_m = 9.16^0 C$	Logarithmic mean temperature difference between working units of generator: $(\Delta\theta)_m = 20.57^0 C$
Convective heat transfer coefficient on the refrigerant (ammonia): $\alpha_o = 668.27W/m^2 \cdot K$	Convective heat transfer coefficient on the refrigerant (freon): $\alpha_o = 821.12W/m^2 \cdot K$	Convective heat transfer coefficient on the refrigerant (freon): $\alpha_o = 850.25W/m^2 \cdot K$
Convective heat transfer coefficient on the ice slurry: $\alpha_{gb} = 295.92W/m^2 \cdot K$	Convective heat transfer coefficient on the ice slurry: $\alpha_{gb} = 497{,}28W/m^2 \cdot K$	Convective heat transfer coefficient on the ice slurry: $\alpha_{gb} = 510.50W/m^2 \cdot K$
Overall heat transfer coefficient: $k = 183.55W/m^2K$	Overall heat transfer coefficient: $k = 211.86W/m^2K$	Overall heat transfer coefficient
The total area of heat transfer between agencies working in generator: $S = 0.68\,m^2$	The total area of heat transfer between agencies working in generator: $S = 3.60\,m^2$	The total area of heat transfer between agencies working in generator: $S = 1.32m^2$
The outer tube diameter: ϕ 245 x 7	The outer tube diameter: ϕ 260 x 6	The outer tube diameter: ϕ 260 x 6
Inner tube: ϕ 219 x 6	Inner tube: ϕ 245 x 7	Inner tube: ϕ 245 x 7
Diameter rotor: $d_{rotor} = 0.160\,m$	Diameter rotor: $d_{rotor} = 0.120\,m$	Diameter rotor: $d_{rotor} = 0.120\,m$
Blade height: $h_{lamela} = 0.023\,m$	Blade height: $h_{lamela} = 0.055\,m$	Blade height: $h_{lamela} = 0.055\,m$
Height screw: $h_{snec} = 2.60\,m$	Height screw: $h_{snec} = 1.01m$	Height screw: $h_{snec} = 1.81m$

Schematic diagram of the binary ice generator with ammonia is shown in figure 2.

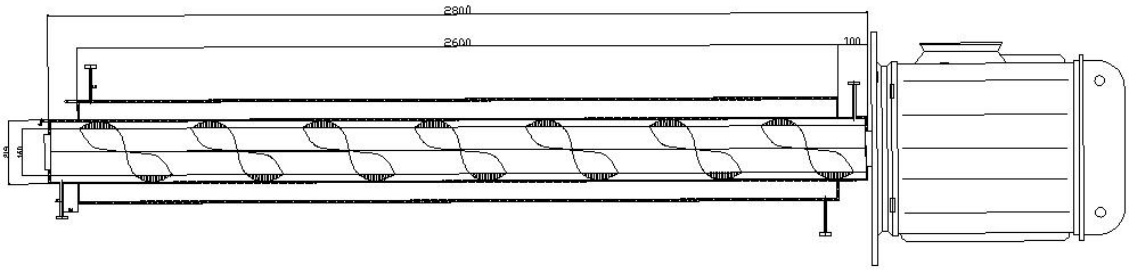

Figura 2. Binary ice generator tube type ammonia pipe surface scrape

3. CONCLUSIONS

Type binary ice generator scrape surface with ammonia, was executed by a team of Department of Machine Building of the Faculty of Machine Technology, headed by Prof. Petre Pătruț. Following the experiments was observed that at low temperatures of binary mixture (less than -5°C), the phenomenon of freezing of the liquid reached the bottom of the spiral leak, blocking the operation of the rotor. Ammonia refrigerator made in the Research Laboratory of the Department of Thermotechnics U.T.C.B., did not give conclusive results.

Given that the market is not functioning refrigeration ammonia with power so we opted to purchase a small generator with binary ice cooling power of 7 kW, the smallest version, available on the market for a research laboratory.

Comparative analysis of calculation results vs. experiment shows that the experimental cooling power generator with freon is greater than the theoretical results of the calculation. This can be explained by the fact that the temperatures of vaporization and hence differences between the temperature of the logarithmic average work differently.

4. REFERENCES

[1] Protocolul de la Kyoto la Convenția-Cadru a Națiunilor Unite asupra Schimbărilor Climatice, 11 decembrie 1997.

[2] Dragoş Hera, Liviu Drugheanu, Alina Girip - Scheme şi cicluri frigorifice pentru instalații cu comprimare mecanică, Editura Matrix Rom Bucureşti, 2002.

[3] ASHRAE Handbook Fundamentals, 2005.

[4] Rodica Dumitrescu, Anica Ilie, Florea Chiriac - Studiu Teoretic şi Experimental privind utilizarea de Ice-Slurry în Instalațiile de Climatizare de Confort, - Universitatea Tehnică de Construcții București, Facultatea de Instalații.

[5] O. Bel - Thermal Study of an Ice-Slurry used as Refrigerant in a Cooling IIF - Commissions, Denmark, 1996;

[6] Paul, L. Malter, U. Munster - Generation and Utilization of Liquid Ice (binary ice) - I.I.R. 20th International Conference on Refrigeration into the Third Millenium, Sydney, Australia, 19 – 24 september 1999.

[7] Stand experimental pentru studiul şi cercetarea proceselor termo – hidraulice şi a echipamentelor din sistemele frigorifice, de aer condiționat şi pompe de căldură – PN II – Capacități, 2007÷2009, responsabil contract: conf. dr. ing. Anica Ilie

[8] Gheața binară - soluție alternativă, energetic şi ecologic, în climatizarea de confort – CNCSIS GR19/2007, 2007÷2008, responsabil contract: conf. dr. ing. Rodica Dumitrescu

[9] Cercetări privind utilizarea amoniacului ca agent ecologic în sisteme frigorifice cu generatoare de gheață binară (ice-slurry) şi acumulare de frig, contract nr. 122/23.12.1999 – RELANSIN, responsabil contract: prof. dr. ing. Florea Chiriac

[10] Chiriac, Fl.: Instalații Frigorifice, Editura Didactică şi Pedagogică, București, Romania,1981.

MULTICRITERIA ANALYSIS OF REFRIGERANT GEOTHERMAL HEAT PUMPS

Ionel OPREA

DEPARTMENT OF THERMAL SYSTEMS AND ENVIRONMENTAL ENGINEERING
"DUNĂREA DE JOS" UNIVERSITY OF GALAȚI

Rezumat: Lucrarea sintetizeaza impactul proprietăților termo-fizice asupra alegerii agentilor frigorifici pentru pompele termice - R600, R404a, R407c, R410a, R134a, R507, R134a şi R717, care au ODP zero. Factorii de impact nu sunt suficienti pentru o evaluare completă, iar o abordare multicriteriala permite o apreciere inițială eficientă a agentilor frigorifici. Parametrii suplimentari, cum ar fi eficiența sistemului şi aspectele legate de siguranță, vor fi incluşi în analiza detaliată.
Cuvunte cheie: pompă de căldură, analiză multicriterială, căldură geotermală

Abstract: This paper summarizes the impact of thermo-physical properties on refrigerant selection for HP: R600, R404a, R407c,R410a, R134a, R507, R134a and R717, which have zero ODP. Impact factors are not sufficient for a complete evaluation, whereas the multicriteria approach allows for an effective initial assessment of the refrigerant. Additional parameters such as efficiency and safety issues will be included in the detailed analysis.
Keywords: heat pump, multicriteria analysis, geothermal heat

1. INTRODUCTION

The choice of a Refrigerant implies compromises between conflicting desirable thermophysical properties. A refrigerant must satisfy many requirements, some of which do not directly relate to its ability to transfer heat. Chemical stability under the conditions of use is an essential requirement. Safety codes may demand for a nonflammable refrigerant of low toxicity for some applications. The environmental impact of refrigerant leaks must also be considered. Cost, availability, efficiency, and compatibility with compressor lubricants and equipment materials are other concerns.

Transport properties (e.g., thermal conductivity and viscosity) affect the performance of heat exchangers and piping system. High thermal conductivity and low viscosity are desirable. No single fluid satisfies all the attributes desired of a refrigerant; consequently, various refrigerants are used.

Table 1. Refrigerant Atmospheric Lifetime, ODP and GWP values

Refrigerant	Atmospheric Lifetime, years[a]	ODP[b]	GWP^{c}_{100}
R-600	0,018[d]	0	~20[d]
R-717	0,01[d]	0	<1[d]
R-134a	14	0	1430

[a] Atmospheric lifetimes from Table 2.14 of 1PCC (2007b) except where indicated;
[b] ODP from UNEP (2006), Section 1.1, Annexes A, B, and C, pp. 23-25;
[c] GWP_{100} from Table 2.14 of IPCC (2007b) except where indicated;
[d] Calm and Hourahan (2007).

Refrigerant blend	ODP*	GWP_{100}*
404A	0	3900
407C	0	1800
410A	0	2100
507A	0	4000

*ODPs and GWP_{100}s from Calm and Hourahan (2007), computed based on mass-weighted average values for individual components

High heat of evaporation is beneficial, as used to achieve a certain cooling (or heating) capacity. However, it is important to note that the mass flow is determined by the swept volume flow of the compressor and by the density of the refrigerant. It is therefore of interest to compare the product of the heat of vaporization and the density of the refrigerant vapour as it enters into the compressor, as this product gives an indication of the capacity

achieved with a specific compressor (i.e., a specific volume flow).

2. HEAT PUMP SYSTEM

There are various technical models of heat pumps. The most advanced technical and commercial designs are the compression and absorption heat pumps. The compression heat pumps have a COP many times higher than that of the absorption versions. A simplified heat pump system consists of four major components, namely compressor, condenser, expansion valve and evaporator.

Assuming a heat pump cycle starts at the compressor outlet, it goes through a condenser, an expansion valve, an evaporator and comes back to the compressor inlet to complete a cycle. This cycle can be represented by a pressure-enthalpy diagram (p-h diagram) as shown in Figure 1, below. All values correspond to the refrigerant's temperature under operating conditions (e.g., 70°C, 60°C, 52°C, 45°C condensing temperature and 0°C evaporating temperature).

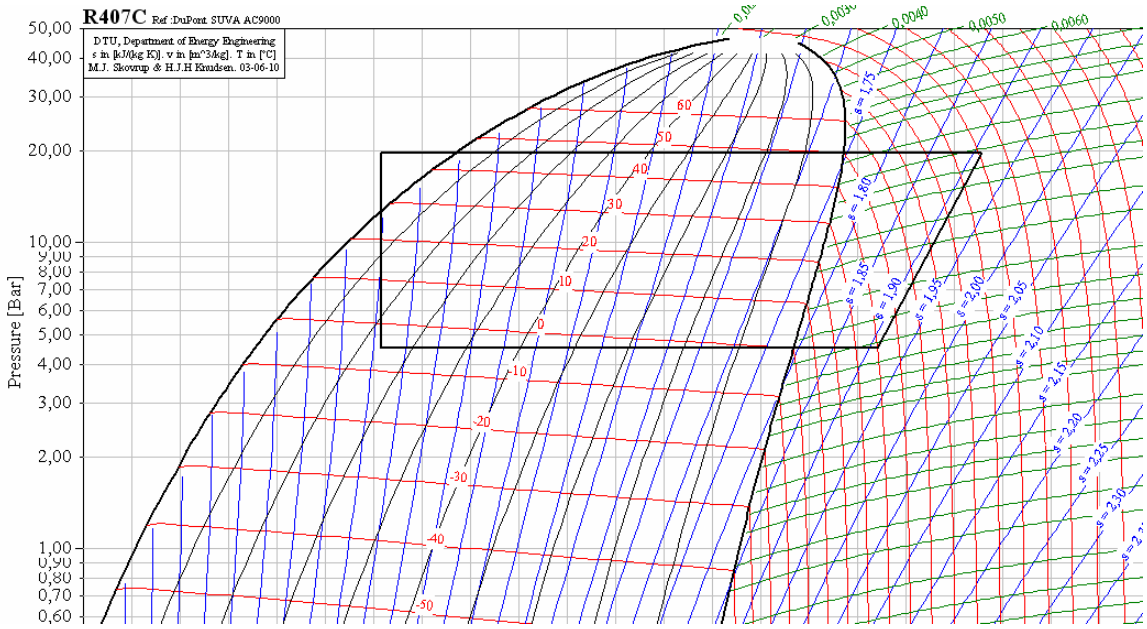

Fig. 1 Representation of refrigerant cycle for a zeotropic refrigerant

3. COMPARATIVE ANALYSIS

This paper has investigated the properties of hydrocarbon butane R600, R404a, R407c,R410a, R507, R134a and ammonia. It is shown that the properties of hydrocarbon make them suitable as refrigerants and that the system's efficiencies should be expected to be equal to, or higher than, those of R404a, R717, and R134a systems. The risks represented by the flammability of the hydrocarbons must be seriously taken into account. The risks can be reduced by designing the systems for a minimum charge of refrigerant, careful leak detection during production, hermetic design with a minimum number of connections, the use of spark-proof electric components and ventilation of confined spaces.

The following matters are taken into account in this multicriteria analysis:

1. **COP - coefficient of performance**: refrigerants with a high critical temperature give the best COP; the natural refrigerants are superior in this respect.

2. $\mathbf{q_k}$: in HP cycles involving condensation, a refrigerant must be chosen so that this change of state will occur at a temperature somewhat below the critical temperature;

3. $\mathbf{q_0}$: since the evaporation of the liquid is the only step in the HP cycle which produces heating, the latent heat of a refrigerant should be as high as possible. Considering condensation and evaporation, ammonia (R717) is a better heat conductor, compared with the synthetic refrigerants.

4. **V - swept volume flow**: compressors are often some of the most critical and expensive systems at a production facility, and deserve special attention.

5. **W - compressor work**: for the efficiency of the process the compressor work is also of interest. The compressor work of isentropic compression from the temperature of 0°C to 70°C, 60°C, 52°C,

45°C to the condensing temperature, is given for the different fluids.

6. **H - compression ratio**: when operating between two specific temperatures, fluids with low vapour pressures (high normal boiling point) will have larger compression ratios than fluids with high vapour pressures. However, there are exceptions to this general rule and this can be clearly seen in the comparison.

Table 2. Numerical results for comparative analysis

Agent	Cycle	COP	q_k [kJ/kg]	q_0 [kJ/kg]	V [m^3/kg]	W [kW]	H [/]	ODP	GWP	Price per unit [$]
R404a	0/15/45	5.132	135.605	109.1857	144.1377	3.012	3.392=20.446/6.028	0	3900	234
	0/15/52	4.188	124.703	94.93	144.137	3.691	3.984=24.018/6.028			
	0/15/60	3.288	109.812	76.4137	144.1364	4.702	4.754=28.66/6.028			
R407c	0/15/45	5.57	198.252	162.717	226.4271	2.774	3.822=17.275/4.52	0	1800	299
	0/15/52	4.697	189.393	149.0768	226.427	3.291	4.55=20.59/4.52			
	0/15/60	3.905	177.753	132.245	226.4268	3.959	5.522=24.959/4.52			
R410a	0/15/45	5.24	193.921	156.9683	145.4327	2.946	3.382=27.014/7.986	0	2100	219
	0/15/52	4.347	182.679	140.66	145.4696	3.556	3.975=31.745/7.986			
	0/15/60	3.499	166.665	119.0368	145.4696	4.418	4.747=37.908/7.986			
R507	0/15/45	5.38	142.541	116.05216	136.0246	2.873	3.373=21.186/6.282	0	4000	255
	0/15/52	4.463	133.971	103.961	136.0238	3.463	3.97=24.94/6.282			
	0/15/60	3.56	120.683	86.835	136.0238	4.336	3.97=29.884/6.282			
R600	0/15/52	5.22	347.6	254.1757	1540.189	3.028	4.606=7.267/1.578	0	20	172
	0/15/60	4.473	335.574	232.783	1540.1874	3.561	5.572=8.792/1.578			
	0/15/70	3.758	319.233	213.47	1540.1842	4.062	6.534=10.309/1.578			
R717	0/15/52	5.11	1311.437	1054.9183	1239.0119	3.024	4.985=21.407/4.294	0	1	86
	0/15/60	4.44	1310.118	1015.13	1239.0116	3.481	6.088=26.143/4.294			
	0/15/70	3.813	1306.421	979.4127	1239.011	3.882	7.712=30.894/4.294			
R134a	0/15/52	4.916	171.256	136.417	296.9971	3.145	4.73=13.851/2.928	0	1430	129
	0/15/60	4.154	162.769	123.5823	296.9986	3.722	5.74=216.813/2.928			
	0/15/70	3.4	150.937	111.8546	296.9971	4.278	6.754=19.777/2.928			

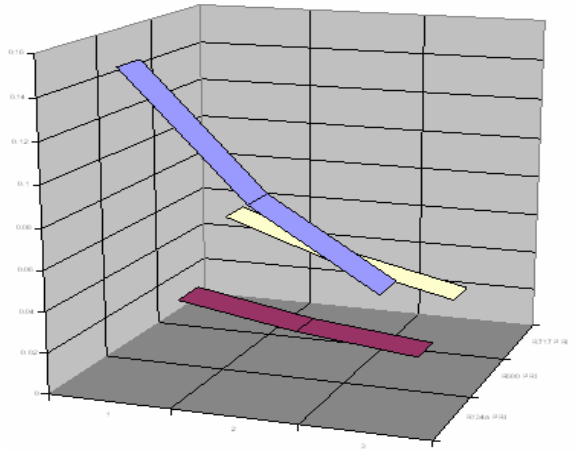

Fig. 2 Comparative analysis of R600, R134a and R717 (70°C, 60°C, 52°C, condensing temperature and 0°C evaporating temperature)

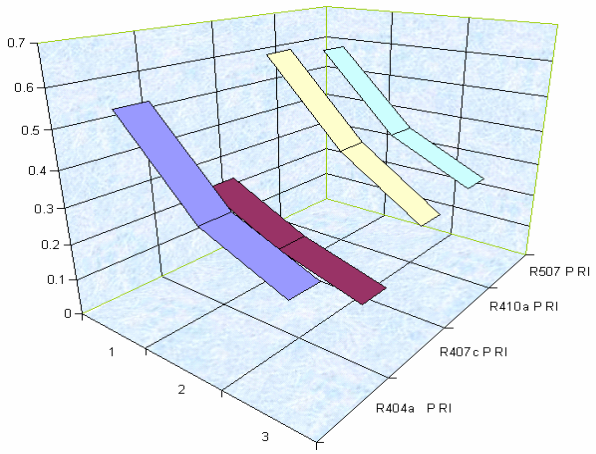

Fig. 3 Comparative analysis for R404a, R407c, R410a, R507 (60°C, 52°C, 45°C condensing temperature and 0°C evaporating temperature)

7. **ODP ozone depleting potential**: the fact that these ‘‘harmless’’ substances were found to have a very unexpected and harmful impact on the global environment, raised doubts also about the use of other manmade substances, not present in the natural environment. Later, these doubts have been confirmed by the fact that the emissions of these refrigerants contributed by more than 20% to the global release of CO_2 - equivalents during some years before the ban of the CFCs (IPCC/TEAP, 2005)

8. **GWP - global warming potential**: the refrigerant selection based on a simple approach of ‘zero ODP’ will have to pay high costs to both global warming and energy efficiency. Using this single criterion is no longer environmentally acceptable today.

9. **Price per Unit of refrigeran**t.[$]

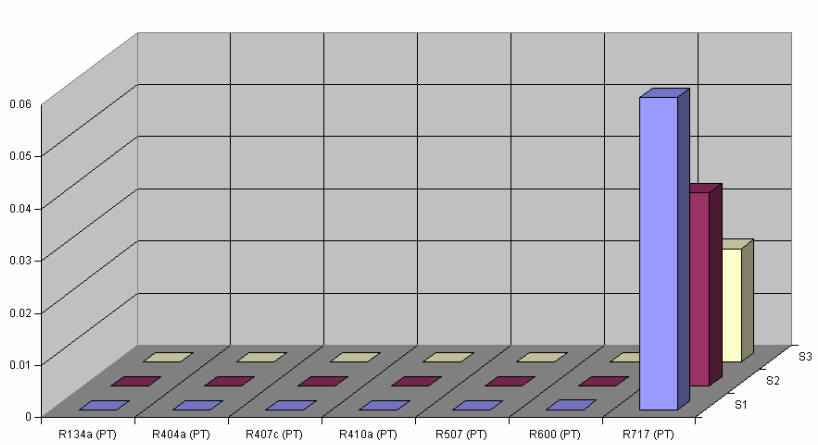

Fig. 4 Comparative analysis (70°C, 60°C, 52°C, 45°C condensing temperature and 0°C evaporating temperature)

4. CONCLUSION

The evaporation heat content of R404a is significantly lower (90% less) than the baseline R717 value, while that of R410a is slightly higher. The COP cycle of R134a is about 17% lower than the baseline value, indicating that this refrigerant does not match the baseline R407c cycle performance. These characteristics imply that both R404a and R410a refrigerants have weaker heat transfer ability and lower cooling capacity on equal heat pump load base, as compared to R717.

Increased vapor density for R507, R410a and R404a may also lead to the use of a smaller compressor and coil tubing that could result in less system power consumption and more efficient component design.

Overall, however, a comparable COP system is possible for R404a, and even a moderate system efficiency improvement might be expected for R410a for a certain heat pump load. The COP system is also influenced by compressor volumetric efficiency, which is a function of compression ratio H (p_{cond}/p_{evap}) and compressor isentropic efficiency, which could be affected by other transport properties, as well as system design.

Nomenclature

COP - coefficient of performance
qo - heat of vaporization (kJ/kg)
qk - heat of condensation (kJ/kg)
pk - condensing pressure (bar)
po - evaporation pressure (bar)
W - compressor work (W)
V - volume flow (m^3/s)

REFERENCES

[1]. UNEP. 1998. 1998 Report of the Refrigeration, Air Conditioning and Heat Pumps Technical Options Committee, Nairobi,

[2]. AFF. 2001. Conseil National du Froid – *Livre blanc sur les fluides frigorigènes*, Paris, AFF, 51 pages.

[3]. UNEP. 2000. Report of the Technology and Economic Assessment Panel April 2000, Nairobi, UNEP, 193 pages

[4]. Harnisch J, Hendriks C. 2001. Economic Evaluation of Emission Reductions of HFCs, PFCs and SF in Europe, Ecofys Energy and Environment.

[5]. Chang,Y.S., Kim, M.S., Ro, S.T., 2000.Performance and heat transfer characteristics of hydrocarbon refrigerants in a heat pump system. International Journal of Refrigeration 23 (3), 232–242.

[6]. Pelletier, O., 1998. Propaneas Refrigerant in Residential Heat Pumps. Licentiate thesis. Royal Institute of Technology, Stockholm, Sweden, ISSN 1102-0245, ISRN KTH/REFR/R-98/24-SE.

THEORETICAL RESEARCH CONCERNING THE TEMPERATURE FIELD INSIDE AN ARTIFICIAL SKATING RINK

Gelu COMAN, Tănase PANAIT, Marcel DRĂGAN

"Dunărea de Jos" University of Galați, Romania

Rezumat. Lucrarea prezintă studiu transferului de căldură şi formarea gheţii în jurul ţevilor pistei unui patinoar, utilizând metoda elementului finit.Distribuţia temperaturii în timpul formării gheţii în jurul tevii din pista patinoarului nu poate fi modelată utilizând metode analitice.Lucrarea przintă o metodă de calcul pentru distribuţia temperaturii în jurul ţevilor.Transferul de căldură în pista patinoarului este nestaţionar şi cu schimbare de fază.
Cuvinte cheie. solidificare, gheaţă, pista patinoarului, schimbare de fază.

Abstract. The paper describes a model for heat transfer and ice formation around the pipes of an artificial skating rink using finite element method. For pipe classifier ice rinks, temperature distribution during ice formation cannot be modeled using analytical methods. The paper presents a method for computing the temperature distribution around the pipes. Heat transfer in ice rink track is unsteady and involves phase change.
Keywords. solidification, ice, skating rink, heat transfer, phase change.

1. Introduction

The problem of melting and solidification of substances, regarded from the point of finding the temperature distribution within solid and liquid phases and of the movement of the solid – liquid interface, is very interesting (both from theoretical and practical point of view), because conduction heat transfer accompanied by phase change occurs in many applications, such as ingots solidification, directional solidification of alloys in order to obtain a certain metallographic structure, freezing of foods, soil freezing and thawing, phase change thermal storage, etc. Mathematical modeling of this phenomenon and especially mathematical solving of this problem are aggravated by the fact that general solutions refers to unsteady 3D temperature distribution for bodies whose thermo-physical properties depend on temperature.[1, 2]

2 Problem Formulation

Numerical modeling was accomplished using Fluent 6.3, software for two different constructive types of the ice rink track: track with pipes immersed in water and pipes embedded in sand. For symmetry reasons, the study was performed using a plane discretization grid, bounded as follows: to the left and to the right by two vertical axis in the middle of the distance between the two adjacent pipes, on top, a horizontal line representing the water (or ice) surface, and another one the bottom for the foundation plate (Fig 1.).

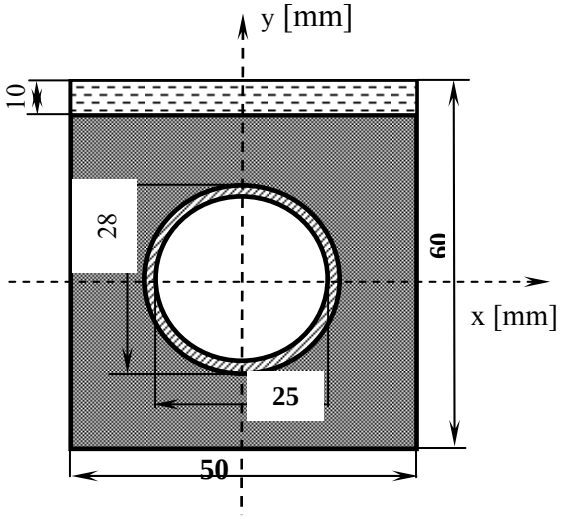

Fig.1 *Sand embedded pipe domain*

For water immersed pipe, the boundary of the computing domain are the same as shown above, with the remark that the entire surface around the pipe was considered as liquid. For this case, the grid contains 13563 mesh points and 12952

tetrahedral elements, and for the second case 11243 mesh points and 10896 de elements.

Due to the multiblock structurated gridding using tetrahedral elements, the grid has a relatively small number of elements, fact that has a positive influence on computational time, on solution convergence and on results accuracy.

Fluent software has an impressive library with properties of various solid and fluid substances [6]. Numerical modeling of phase change heat transfer using this software is consistent with the real solidification process around cylindrical surfaces. The transport properties of the substances are now temperature dependent, and the phase change is non isothermal.

The chosen mathematical model is Pressure Based, considering that heat transfer occurs in incompressible fluids. The model is considered implicit that makes the solver stable and convergent, although the number of equations increases and therefore the complexity of computations. The implicit scheme is recommended for phase change heat transfer, for the reason that offers the liberty of choosing the time step in a large range.

The chosen solver type was *Solidification and melting*, solver that is intended for this type of problems. For a better analysis of temperature distribution, in certain areas were added some points and contours in which was tracked the temperature variation during the process (Fig. 2). At the same time, the temperature variation was also tracked on several important surfaces such as: water surface, foundation slab and pipe inner/outer surface.

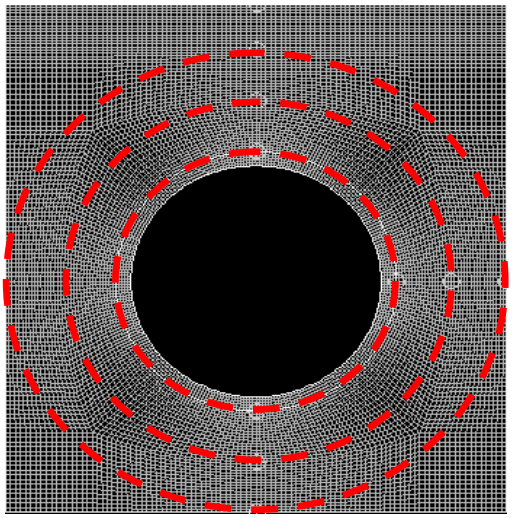

Fig.2 *The grid of the analyzed domain*

The equations of the mathematical model [3] and initial and boundary conditions are:

$$\frac{\partial \rho}{\partial \tau} + \nabla(\rho V) = 0 \quad (1)$$

$$\frac{\partial(\rho u)}{\partial \tau} + \nabla(\rho u V) = -\frac{\partial p}{\partial x} - \frac{\mu}{k} u + \nabla(\mu \nabla u) \quad (2)$$

$$\frac{\partial(\rho v)}{\partial \tau} + \nabla(\rho v V) = -\frac{\partial p}{\partial y} - \frac{\mu}{k} v + \nabla(\mu \nabla v) + (\rho_m - \rho) g \quad (3)$$

$$\frac{\partial(\rho h)}{\partial \tau} + \nabla(\rho h V) = \nabla\left(\frac{k}{c} \nabla h\right) - \frac{\partial(\rho \beta L)}{\partial t} - \nabla(\rho \beta L V) \quad (4)$$

$$K = K_0 \left(\frac{\beta^3}{(1-\beta)^2} \right) \quad (5)$$

where:

τ - time, ρ - density, p - pressure, V - velocity vector, u, v - velocity components on x and y axes, μ - dynamic viscosity, β - liquid fraction, L - latent heat, K - permeability, K_0 - Kozeny-Carman constant.

$$h = \begin{cases} C_s T & T < T_f \\ C_l T & T \geq T_f \end{cases} \quad (6)$$

$$h = h_{ref} + \int_{T_{ref}}^{T} c_p dT \quad (7)$$

where:

T_f - solidification temperature, C_s, C_l -specific heat of solid and liquid phase, h - enthalpy, T_{ref} - reference temperature, h_{ref} - reference enthalpy, c_p - constant pressure specific heat.

3 Problem Solution

For the numerical simulation of ice formation around water immersed pipe, were performed 25210 iterations using a time step τ = 10 seconds. The total time for the solidification process was 7 hours, and the process was considered ended when free surface of ice reached a temperature of -5.55 °C

For the sand embedded pipe were performed 18000 iterations using a time step of 10 s. The total time for the solidification process was 5 hours, and the process was considered ended when free surface of ice reached a temperature of -4.62 °C.

Parameters of the mathematical model were:

- initial water temperature t_{water} = 10 °C
- surrounding air temperature t_{air} = 10 °C

- refrigerant temperature inside the pipe t_r = -10 °C
- refrigerant flow rate $\dot{m}$ = 0.185 kg/s
- refrigerant convection coefficient inside the pipe α_{agent} = 550 W/m^{2}K
- air convection coefficient at the water surface α_{aer}= 15W/m^{2}K
- heat flow rate for the base plate q = 10W/m^2.

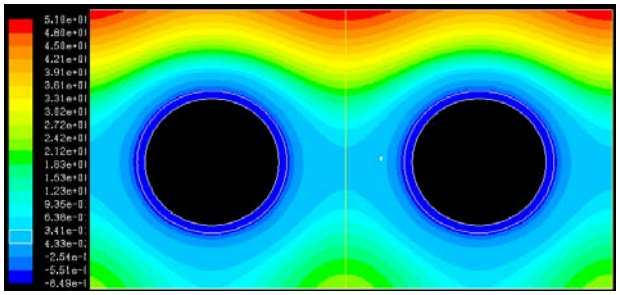

Fig.3 *Temperature distribution at τ = 30min*

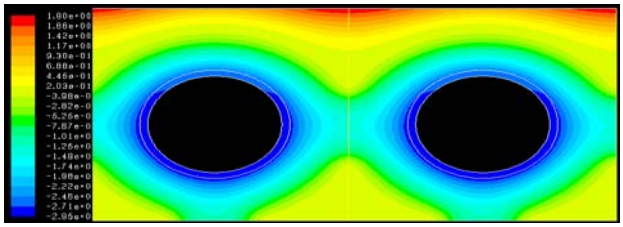

Fig. 4 *Temperature distribution at τ = 150 min*

In Fig. 3 and 4 are shown pictures of temperature distribution over time for the water immersed pipe. It can be noticed the different distribution over the 2 axis, due to different boundary conditions and also due to external influences. Thus, for the *X* and *–Y* directions we have a swift temperature decrease, and on *Y* direction a slower decrease due to the water surface convective heat flow.

A special importance for ice formation on the outer surface of the pipe process is time variation of the solidification rate.

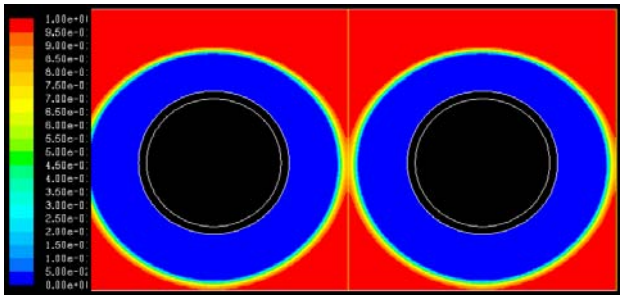

Fig.5 *Liquid fraction distribution for τ = 120 minutes*

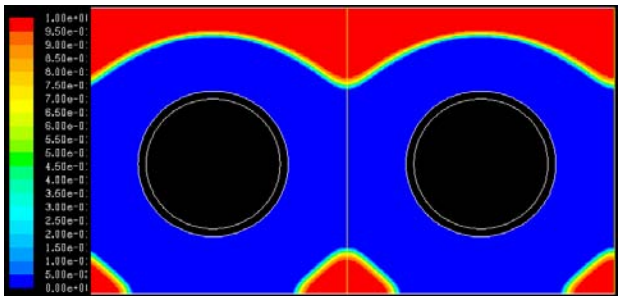

Fig.6 *Liquid fraction distribution for τ = 180 minutes*

Fig. 5 and 6 are shown pictures of the solidification front for some moments in time.
Ice formation process around the pipes ends at τ = 296 minutes, moment at which the liquid fraction for the entire domain becomes zero, and the solid one becomes one.
During solidification it can be noticed a differential increase of solidification rate around the pipe: a rapid increase on the sides and on the bottom of the pipe (τ = 180 minute) and a slow increase on the top.

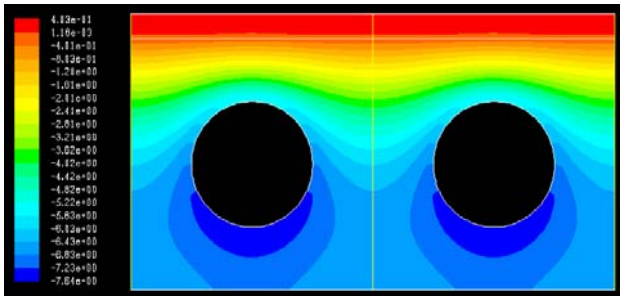

Fig.7 *Temperature distribution at τ = 30min*

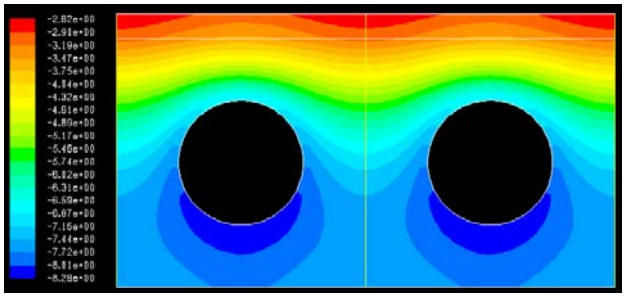

Fig.8 *Temperature distribution at τ = 120min*

Fig. 7 and 8 show images of temperature distribution for the sand embedded pipe for some moments in time.

In comparison to the water immersed pipes, it can be noticed a steeper temperature decrease on

the domain surfaces and a more uniform distribution on the air-water contact surface.

At the end of the process, minimal temperatures on the envisaged surfaces were as follows:

- inner pipe temperature t = -8,4 ^{0}C
- bottom plate temperature t = -8,32 ^{0}C
- sand-water contact surface temperature t = -5,15 ^{0}C
- ice surface temperature t = -4,62 ^{0}C

Fig. 9 and 10 illustrate the time variation of the water surface temperature in the two cases analyzed: tube submerged in the water and pipe buried in sand. When immersed in water (Figure 9) there is a sharp decrease in temperature in the nodes above the pipe and a slower decrease in the points located midway between the pipes. Under isothermal 0 ^{0}C after τ = 300min, there is an almost constant distribution in nodes.

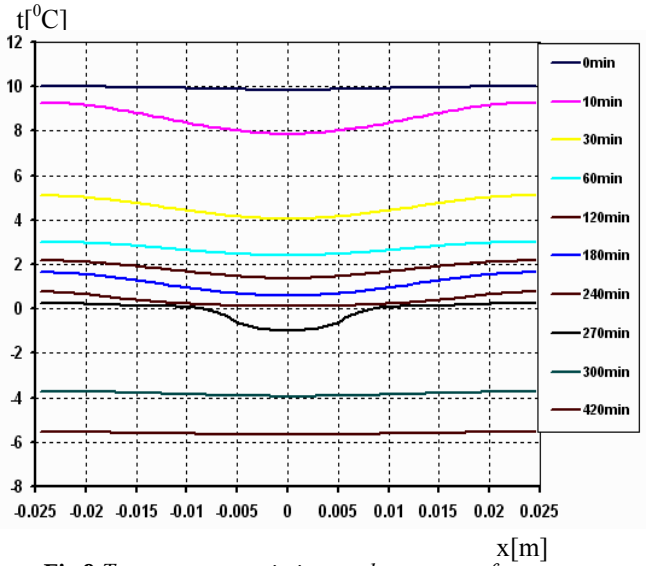

Fig.9 *Temperature variation on the water surface at pipe submerged in water*

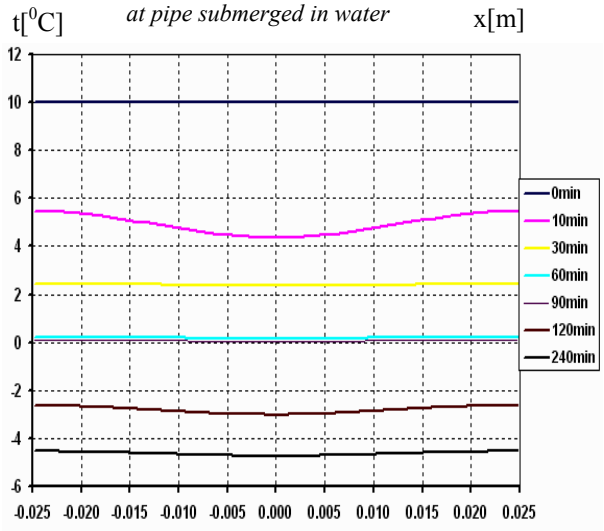

Fig.10 *Temperature variation on the water surface at pipe buried in the sand*

4 Conclusion

Analyzing the presented data it results that from heat transfer and ice quality point of view the sand embedded pipe design is preferable due to the following advantages:

- total solidification time of water is shorter;
- temperature distribution on water surface is more even, thus obtaining a higher quality of ice;
- propagation of the solidification front is swift and uniform on the entire domain;
- a more uniform temperature distribution on the pipe inner surface, i.e. an intensified heat transfer from the refrigerant to the ice rink track.

REFERENCES

[1] LEWIS R.W., ROBERTS P.M. - *Finite element simulation of solidification problems*. App. Scientific Research, Vol. 44, pp 61-92,1987.

[2] SASAGUCHI K., VISKANTA R. - *Phase-change heat transfer during melting and resolidification of melt around cylindrical heat source(s)/Sinks*, Jl. of Energy Resources Technology, vol.111, 1989

[3] Shih Y,Chou H, *Numerical study of solidification around staggered cylinders in a fixed space*, Numerical Heat Transfer, No.40, 1997,pp 1343-1354

[4] Vick B, Nelson DJ, Yu X, *Model of an ice-on-pipe brine thermal storage component*, ASHRAE Trans, No.102,1996, pp 45-54.

[5] Vick B, Nelson DJ, Yu X, *Freezing and melting with multiple phase fronts along the outside of a tube*, J Heat Transfer, No.120 (1998), pp. 422-429

[6] FLUENT Inc, Fluent user's guide, 2003.